Department of Electrical Engineering

Dovetail rotor poles in synchronous permanent magnet and reluctance machines

Jere Kolehmainen

Aalto University

DOCTORAL DISSERTATIONS

Aalto University publication series
DOCTORAL DISSERTATIONS 60/2011

Dovetail rotor poles in synchronous permanent magnet and reluctance machines

Jere Kolehmainen

Doctoral dissertation for the degree of Doctor of Science in Technology to be presented with due permission of the School of Electrical Engineering (Espoo, Finland) for public examination and debate in Auditorium S1 at the Aalto University School of Electrical Engineering (Espoo, Finland) on the 9th of September 2011 at 12 noon.

Aalto University
School of Electrical Engineering
Department of Electrical Engineering
Electromechanics

Supervisor
Prof. Antero Arkkio

Preliminary examiners
Prof. Nicola Bianchi, University of Padova, Italy
Prof. Chandur Sadarangani, Royal Institute of Technology, Sweden

Opponent
Prof. Zi-Qiang Zhu, University of Sheffield, UK

Aalto University publication series
DOCTORAL DISSERTATIONS 60/2011

ISBN 978-952-60-4195-7 (pdf)
ISBN 978-952-60-4194-0 (printed)
ISSN-L 1799-4934
ISSN 1799-4942 (pdf)
ISSN 1799-4934 (printed)

Aalto Print
Helsinki 2011

Finland

The dissertation can be read at http://lib.tkk.fi/Diss/

Author
Jere Kolehmainen

Name of the doctoral dissertation
Dovetail rotor poles in synchronous permanent magnet and reluctance machines

Publisher School of Electrical Engineering

Unit Department of Electrical Engineering

Series Aalto University publication series DOCTORAL DISSERTATIONS 60/2011

Field of research Electromechanics

Manuscript submitted 31 March 2011 **Manuscript revised** 28 June 2011

Date of the defence 9 September 2011 **Language** English

☐ **Monograph** ☒ **Article dissertation (summary + original articles)**

Abstract

Robust synchronous permanent magnet and reluctance machine designs are developed. In the designs, the rotor structure is simple and strong and the leakage flux is relatively small. For the new design solution, a dovetail form-blocked rotor structure, specific analyzing principles are also developed.

The dovetail designs are shown to be good solutions with their lower leakage flux and at least the same strength against centrifugal forces as the conventional rotor solutions. The compared conventional solutions considered have inseparable rotor sheets in which the parts of the rotor are kept still by using bridges between them. In the dovetail rotor, the forms of the rotor parts keep them together and no bridges between them are needed for support. The simplicity of the dovetail solution has also been kept the same or better. In addition, the manufacturing method is the same for both solutions. The dovetail design can also be used for saving the magnetic material of permanent magnet synchronous machines because it has a smaller leakage flux than the conventional V-shaped designs with supporting bridges.

The problem of how to compare the dovetail designs to the conventional ones is considered in depth. The strength of the dovetail structure has to be defined in a different way than in the conventional design with supporting bridges. In bridge-fixed design, the strength of the bridges is critical for rotor durability but in the dovetail design wider areas of the rotor affect the strength of the rotor. However, the basic electrical properties could be defined with the same method. Additional methods for defining the electrical properties of dovetail designs are also considered. One method is that the load angle can be defined only from the forms of phase currents in delta-connected synchronous machines and phase voltage and current in star-connected synchronous machines. The load angles defined are successfully used to find a good model for the test results. The other method is to view the normalized local torque density in the air gap as a function of time.

In this work, several dovetail synchronous reluctance and permanent magnet machines are designed, manufactured, tested, and analyzed. The design, manufacturing, testing, and analysis methods are defined and developed especially for dovetail designs.

Keywords Electromagnetic analysis, strength analysis, permanent magnet machines, synchronous reluctance machines.

ISBN (printed) 978-952-60-4194-0 **ISBN (pdf)** 978-952-60-4195-7

ISSN-L 1799-4934 **ISSN (printed)** 1799-4934 **ISSN (pdf)** 1799-4942

Location of publisher Espoo **Location of printing** Helsinki **Year** 2011

Pages 132 **The dissertation can be read at** http://lib.tkk.fi/Diss/

Aalto-yliopisto

Tiivistelmä

Aalto-yliopisto, PL 11000, 00076 Aalto www.aalto.fi

Tekijä
Jere Kolehmainen

Väitöskirjan nimi
Muotosuljetut roottorin navat tahtikestomagneettikoneissa ja tahtireluktanssikoneissa.

Julkaisija Sähkötekniikan korkeakoulu

Yksikkö Sähkötekniikan laitos

Sarja Aalto University publication series DOCTORAL DISSERTATIONS 60/2011

Tutkimusala Sähkömekaniikka

Käsikirjoituksen pvm 31.03.2011 **Korjatun käsikirjoituksen pvm** 28.06.2011

Väitöspäivä 09.09.2011 **Kieli** Englanti

☐ **Monografia** ☒ **Yhdistelmäväitöskirja (yhteenveto-osa + erillisartikkelit)**

Tiivistelmä

Tässä työssä on suunniteltu useita uudenlaisia kestomagneettitahtikoneita ja tahtireluktanssikoneita. Näissä koneissa roottorit ovat yksinkertaisia ja vahvoja samalla kun niiden hajavuot ovat suhteellisen pieniä. Käsitellylle uudelle muotosuljetulle roottorin naparakenteelle on myös kehitetty omia analysointimenetelmiä.

Muotosuljettujen rakenteiden on osoitettu olevan hyviä korvaajia tavanomaisille rakenteille, joissa navat ovat kiinni toisissaan roottorilevyihin jätetyillä kannaksilla. Muotosuljetuilla roottoreilla roottorin osien muodot pitävät niitä paikoillaan, eikä kannaksia tarvita. Niillä hajavuot ovat pienempiä ja samalla rakenteet ovat vahvempia kuin tavanomaisilla rakenteilla. Suunniteltujen muotosuljettujen rakenteiden valmistusmenetelmät ovat myös yhtä yksinkertaisia kuin tavanomaisten rakenteiden. Lisäksi kestomagneettikoneilla muotosuljettu rakenne antaa mahdollisuuden säästää magneettimateriaalia johtuen pienemmistä hajavoista verrattuna alkuperäisiin rakenteisiin, joissa vuota johtavat kannakset pitävät paikoillaan napoja ja magneetit ovat aseteltu V:n muotoon.

Työssä on käsitelty syvällisesti sitä kuinka muotosulkeisia rakenteita kannattaa analysoida ja verrata tavanomaisesti käytettyihin rakenteisiin, joissa kannakset pitävät roottorin osia paikoillaan. Muotosuljetun roottorin lujuus täytyy määritellä eri tavalla kuin roottorin, jota kannakset pitävät kasassa. Kannaksellisen roottorin lujuuden määrittävät lähes yksinomaan kannakset, mutta muotosuljetun roottorin lujuuden määrittämiseksi roottorin lujuutta täytyy tarkastella laajemmin. Sähköiset ominaisuudet voidaan määritellä alkuperäisillä menetelmillä, mutta myös uusia menetelmiä muotosuljettujen rakenteiden sähköiseen analysointiin on kehitetty. Yhdessä menetelmässä roottorin kuormituskulma voidaan suoraan määrittää vaihevirroista kolmio-kytketyillä tahtikoneilla ja vaihevirroista ja vaihejännitteistä tähti-kytketyillä tahtikoneilla. Toisessa menetelmässä roottorin ominaisuuksia voi selvittää tarkastelemalla paikallista vääntömomenttitiheyttä ilmavälissä ajan funktiona.

Tässä työssä on myös suunniteltu, valmistettu, testattu ja analysoitu useita muotosuljettuja tahtireluktanssi- ja kestomagneettikoneita. Suunnittelu-, testaus- ja analysointimenetelmiä on kehitetty erityisesti silmälläpitäen muotosuljettuja rakenteita.

Avainsanat Sähkömagneettinen analyysi, lujuus analyysi, kestomagneettitahtikoneet, tahtireluktanssikoneet

ISBN (painettu) 978-952-60-4194-0 **ISBN (pdf)** 978-952-60-4195-7

ISSN-L 1799-4934 **ISSN (painettu)** 1799-4934 **ISSN (pdf)** 1799-4942

Julkaisupaikka Espoo **Painopaikka** Helsinki **Vuosi** 2011

Sivumäärä 132 **Luettavissa verkossa osoitteessa** http://lib.tkk.fi/Diss/

Preface

This research work was carried out during the period between 2004 and 2010 at ABB Oy, Motors. The work was finalized during 2010, partly at the Department of Electrical Engineering, Aalto University.

My deep appreciation is first given to almighty God for blessing me with success in my efforts and blessing me with the several people whose advice, assistance, and encouragement helped me throughout the completion of this dissertation.

I would like to express my sincere gratitude to Professor Antero Arkkio for his encouragement, guidance, and support during the work.

I wish to express my special gratitude to the Product Development Manager of ABB Oy, Motors, Dr. Jouni Ikäheimo, for his enthusiastic attitude towards my ideas about research on electrical machines and for making it possible to write the results up as scientific articles and later as a Doctoral dissertation.

Special thanks to Professor Emeritus Tapani Jokinen. I asked him in 2002 if it was possible to write a dissertation about electrical machines. He explained to me how it would be possible and what was needed for it. After some trial and error, I found my subject in 2004.

I also would like to thank the staff of the product development department and test field at ABB Oy, Motors. Especially, I want to thank Mr. Alpo Hauru for supervising me in the area of electrical designs.

I also would like to thank Dr. Anouar Belahcen for his valuable comments while I was finalizing my writing.

I want to thank Dr. Sami Ruoho for his good cooperation in several publications.

I also would like to thank the Academy of Finland for financial support while I was finalizing my research and writing this dissertation.

I also thank my parents, Jorma and Salme, and my sisters, Jessi and Jetta, for their encouragement during the work.

Special thanks to my son Daniel and daughter Saara for giving me joy during my work.

Contents

List of publications

This dissertation consists of an overview and of the following publications:

P1. Kolehmainen J. Finite element analysis of two PM-motors with buried magnets. International Conference on Electrical Machines – ICEM'04, September 2004. SPRINGER MONOGRAPH "Recent Developments of Electrical Drives," pp. 51-58, November 2006.

P2. Kolehmainen J., Ikäheimo J. Motors with buried magnets for medium-speed applications. IEEE Transactions on Energy Conversion, Vol. 23, No. 1, pp. 86-91, March 2008.

P3. Kolehmainen J. Machine with a rotor structure supported only by buried magnets. International Symposium on Electric Fields in Mechatronics, Electrical and Electronic Engineering – ISEF'07, September 2007. Advanced Computer Techniques in Applied Electromagnetics by IOS Press – Studies in Applied Electromagnetics and Mechanics, Vol. 30, pp. 240-246, 2008.

P4. Kolehmainen J. Optimal dovetail permanent magnet rotor solutions for various pole numbers. IEEE Transactions on Industrial Electronics, Vol. 57, No. 1, pp. 70-77, January 2010.

P5. Kolehmainen J. Permanent magnets synchronous machine with rotor poles supported by magnets. International Conference on Electrical Machines – ICEM'10. September 2010, 6 p.

P6. Kolehmainen J. Synchronous reluctance motor with form blocked rotor. IEEE Transactions on Energy Conversion, Vol. 25, No. 2, pp. 450-456, June 2010.

P7. Ruoho S., Kolehmainen J., Ikäheimo J., Arkkio A. Demagnetization testing for a mixed-grade dovetail permanent-magnet machine. IEEE Transactions on Magnetics, Vol. 45, No. 9, pp. 3284-3289, September 2009.

P8. Ruoho S., Kolehmainen J., Ikäheimo J., Arkkio A. Interdependence of demagnetization, loading, and temperature rise in a permanent-magnet synchronous motor. IEEE Transactions on Magnetics, Vol. 46, No. 3, pp. 949-953, March 2010.

Symbols and Abbreviations

Symbols

B_{m}	Maximum value of the flux density
B_r	Radial component of the flux density
B_φ	Tangential component of the flux density
d	Lamination thickness
f	Frequency
k_{h}	Hysteresis loss coefficient
k_{e}	Excess loss coefficient
$n_{\max}$	Maximum speed
n_{model}	Speed used in the model
r	Radius
T_{e}	Torque per axial length
T	Time for one electric period
σ	Electric conductivity
$\sigma_{\mathrm{modeled}}$	Calculated critical stress
$\sigma_{\tan}$	Local tangential force density
$\sigma_{\tan}^{\mathrm{normalized}}$	Normalized local tangential force density
σ_{yield}	Yield strength
η	Factor of safety

Abbreviations

2D	Two-dimensional
3D	Three-dimensional
Back-EMF	Back electromotive force
FEM	Finite element method
FEA	Finite element analysis
Nd-Fe-B	Neodymium-iron-boron
PM	Permanent magnet
PMASRM	PM-assisted SRM
PMSM	Permanent magnet synchronous motor/machine
SR	Synchronous reluctance
SRM	Synchronous reluctance motor/machine
THD	Time harmonic distortion

1 Introduction

1.1 Overview

This work contributes to the development of robust designs for permanent magnet synchronous machines and synchronous reluctance machines. The main goal is to find a simple rotor structure with the minimum leakage flux and the maximum strength against centrifugal forces at the same time. Another goal is to verify whether the new designs are better than the conventional ones.

The new design solutions considered in this dissertation are dovetail form-blocked rotor designs. In this dissertation, the dovetail designs are shown to have a lower leakage flux and at least the same strength against centrifugal forces as the conventional solution. Additionally, the simplicity of the solution has been kept the same or better. In addition, the manufacturing method remains the same. The dovetail design can also be used for saving permanent magnet material in synchronous machines, because of the smaller leakage flux than in the conventional V-shaped designs with supporting bridges.

The dovetail rotor structures are suggested for use in synchronous permanent magnet (Kolehmainen, 2008a) and reluctance machines (Kolehmainen, 2008b). Examples of eight-pole permanent magnet and four-pole synchronous reluctance machines are shown in Figure 1.

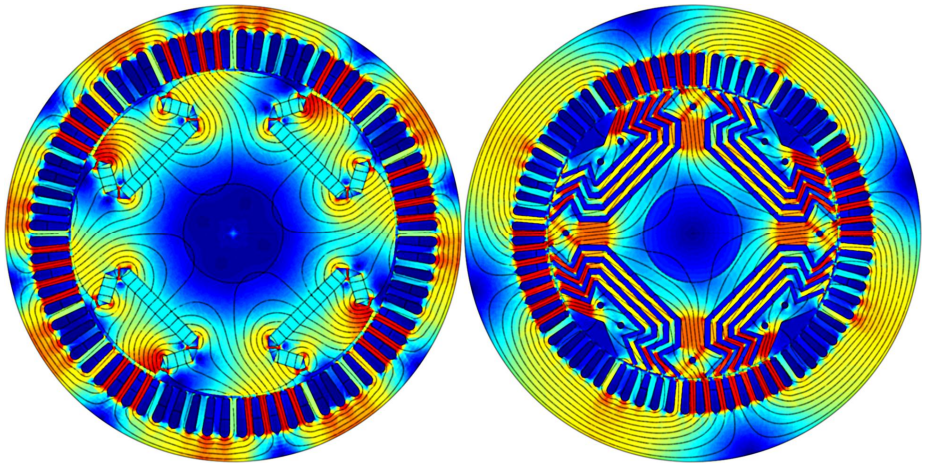

Figure 1: Eight-pole 185-kW and 4000 1/min dovetail synchronous permanent magnet machine (left) and four-pole 90-kW and 1500 1/min dovetail synchronous reluctance machine (right).

This dissertation also considers the problem of how to compare the new dovetail designs to the conventional ones. The strength of the dovetail structure has to be defined in a different way than in the conventional design with supporting bridges. The electrical properties could be defined with the same method. However, additional methods for defining the electrical properties of dovetail designs are also considered.

For strength comparisons, the finite element method is used. Principles for comparing the strengths of very different rotor solutions are developed. The new dovetail rotor structures are developed and compared to the conventional ones. The conventional support method considered in this work is to use the supporting bridges between the poles. The only function of these bridges is to support the rotor structure. Most of the stresses are tension and shear stresses in the bridges and they are relatively easy to model. In the dovetail supporting structures, parts of the rotors under consideration are form-blocked by the magnets, glued magnets, magnets and thin metal sheets, glue, or metal bars. Therefore, important additional physical phenomena in the dovetail structure are the pressure through the magnets, shear stresses between the magnets or the other filler, and forces in the supporting and supported parts of the rotor. The reliability of the dovetail design is proven and analytical methods are developed in this dissertation.

The tested and modeled electrical properties are also compared. The greatest challenge is to define the exact input and output power, voltage, current, and load angle. It is not always so simple and it also depends on the measuring equipment used. In particular, the right load angles are difficult to find out in the measurements. The author shows that the load angle can be defined only from the wave form of phase currents in delta-connected synchronous machines and phase voltage and current in star-connected synchronous machines. The defined load angles are successfully used for finding good model parameters for the test results.

Several dovetail synchronous reluctance and permanent magnet machines are designed, manufactured, tested, and analyzed in this dissertation. Design, manufacturing, testing, and analytical methods are also defined and developed for the dovetail designs.

1.2 Aim of the work

The starting point of this work was to find a new design for rotors of synchronous machines which are more robust against centrifugal forces and, at the same time, have better electrical properties. The dovetail design has been considered for the new design. So, the aim of this work is to prove that the dovetail design is better than the conventional ones by modeling and testing. In addition, the reliability of the new design is shown.

1.3 Scientific contribution

The most important scientific contributions of the study are as follows.

1. The feasibility of the dovetail machine is demonstrated through numerical analysis and actual construction and measurements
2. The mechanical robustness of dovetail-type machines is studied and demonstrated. It is shown that the mechanical robustness does not require any compromise from the magnetic point of view.
3. The magnets can only be installed into every second pole. Asymmetric adjacent poles cause no problems in the machine.
4. The dovetail design is mitigated from PM synchronous machines to synchronous reluctance machines.
5. A method to estimate the load angle of synchronous machines from the phase angles of the fundamental and third harmonics of either the current or the voltage of the machine is developed.
6. The simple mechanical and magnetic design procedure of the dovetail type rotor is presented and confirmed with numerical analysis and through prototyping and measurements.
7. The demagnetization behavior of different PMSMs with mixed- and single-grade poles is measured. It is shown that the mixed grade pole is a potential method to reduce the cost of the machine while keeping good magnetic properties.

1.4 Structure of the work

The dissertation consists of the following parts.

- Chapter 1 presents an introduction and the aim of the work. The scientific contribution and the publications are listed.
- Chapter 2 presents the basic structures of existing synchronous permanent magnets and reluctance machines and their combinations. Only radial flux machines are considered in this dissertation. A literature study of the conflict between the electrical and mechanical properties of synchronous permanent magnets and reluctance rotors is also presented. The structures where the mechanical durability of the magnets is critical are searched for and presented.

- In Chapter 3, the design method, material properties and analysis methods are presented. The usability of mechanical and electrical methods for the dovetail designs is discussed. The new rotor analysis method where the force is analyzed in the stator coordinates is presented, together with a literature study.
- Chapter 4 presents the measuring and measurement analysis methods used in this dissertation. A load angle definition method from the wave form of the phase currents is introduced, together with a literature study.
- Chapter 5 presents the prototypes manufactured and tested during this study.
- The results are discussed and summarized in Chapter 6.

The publications included in this dissertation are reprinted at the end of the dissertation. Chapters 3, 4, and 5 are based on these publications. However, Chapters 4 and 5 also present some important results not included in the publications.

Publication P1

The starting point of the work was the idea that it is possible to include wider magnets in the permanent magnet rotor by inserting three magnets into every second pole. The machine then has a so-called consequent pole rotor. In the structure, there was one magnet installed tangentially at the bottom and two radial magnets at the sides of the poles. In this publication, the electromagnetic properties of the new and conventional V-shaped magnets in every pole are compared by means of the electromagnetic finite element method. The new structure is shown to be useful for including wider magnets and a higher flux concentration.

Publication P2

In order to continue the previous study, the outer ends of the radial magnets can be moved towards the middles of the poles so that the bottom of the pole is wider than the top of the pole. The rotor still has the consequent poles.

The structure is proven to give remarkable support to the poles against centrifugal forces by the mechanical finite element model and the prototype that was tested. The electromagnetic properties are also compared to the structure with V-shaped magnets in every pole. It is shown that both the electromagnetic and the mechanical properties of the permanent magnet machine can be improved by changing the structure with V-shaped magnets in every pole to a structure with dovetail magnets in every second pole. The electromagnetic properties are improved because thinner bridges between the poles can be used in the new structure compared to the conventional one.

This paper was written by Kolehmainen. The co-author, Ikäheimo, contributed to the paper with several discussions and valuable comments. Ikäheimo also created Figure 16 of P2, which compares the vibration levels of the designs being compared.

Publication P3

In this study, the poles are totally separated from each other. There are no bridges between the poles. The structure is proven to be reliable by testing and by analyzing it with the electromagnetic and the mechanical finite element method (FEM).

Publication P4

The effect of the number of dovetail permanent magnet poles on the mechanical and magnetic properties is studied. It is shown that the maximum speed of the dovetail rotor can be increased by increasing the number of poles but the magnetic properties can be improved by reducing their number. The optimum dovetail structure is discussed. Studies are performed by means of mechanical and electromagnetic FEM. The electromagnetic model is also simplified, so that there was a stator without any slots or windings. The results of the three dovetail prototypes (presented in P2, P3, and P5) are compared to the optimized structures.

Publication P5

An improved dovetail design is studied in this study. This structure is also proven to be reliable by testing and analyzing with electromagnetic and mechanical FEM. This dovetail design has two tangential bridges between the poles to make the manufacturing easier. The effects of the dovetail design are analyzed here in depth.

Publication P6

The idea of the dovetail form-blocked structure is extended to synchronous reluctance machines. This structure is studied by testing a prototype and by modeling with electromagnetic and mechanical FEM. The reliability of the structure is discussed.

Publication P7

Demagnetization of mixed-grade magnets is studied with the design introduced in P5. The aim of this study was to get the magnets partly demagnetized in an overheated locked-rotor situation. Pull-outs of the heated machine partly demagnetized the magnets. The demagnetization of the magnets is measured and compared to the modeled results. Two single-grade cases and one mixed-grade one are studied.

This paper was written by Ruoho. Ruoho also developed the demagnetization model, compared the modeled and tested results, and analyzed the partly demagnetized magnets. The first co-author, Kolehmainen, designed and manufactured the prototype rotor and proposed and installed the test setup and the process. Kolehmainen and Ruoho performed the tests together. The other co-authors, Ikäheimo and Arkkio, contributed to the paper with several discussions and valuable comments.

Publication P8

This paper was written by Ruoho. The first co-author, Kolehmainen joined the paper for the results discussed in P7.

2 Brushless synchronous machines

2.1 Synchronous reluctance machines

The process that finally led to the development of synchronous reluctance motors (SRMs) was started by Tesla (1888) by introducing a rotating magnetic field and introducing a machine which is nowadays called a switched reluctance machine. However, a simple and obvious solution for getting a shaft to rotate in a rotating magnetic field is to fix a magnetically non-homogenous part onto the shaft. The first rotating magnetic field synchronous motor was introduced by Kostko (1923). Pure SRMs do not start directly online without a rotor cage. Therefore, earlier SRMs were used with a rotor cage (Lipo and Krause, 1967 and Lipo, 1991). Nowadays, modern inverter technology has created the possibility of starting SRMs without a rotor cage.

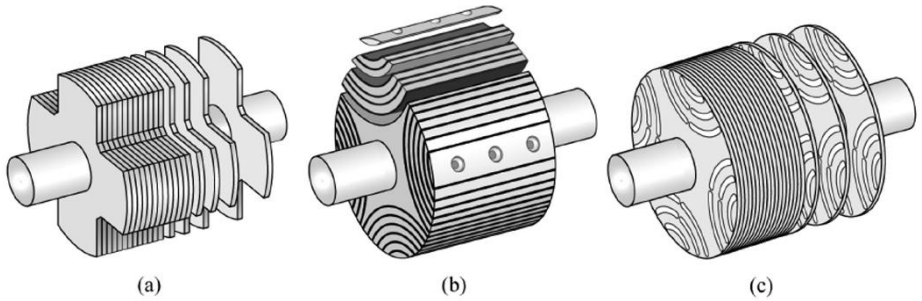

Figure 2: Schematics of: (a) simple salient pole; (b) axially laminated, and (c) transverse laminated rotors (Fukami et al., 2008)

The major types of synchronous reluctance rotors, shown in Figure 2, are the simple salient pole rotor (a) (Lamghari-Jamal et al., 2006), the axially laminated rotor (b) (Cruickshank et al., 1966 and Platt, 1992), and the transverse laminated rotor (c) (Kostko, 1923 and Vagati et al., 2000a). The salient pole rotor design has a simple and rigid structure but a low saliency ratio and consequently poor performance. However, the rigid structure creates the possibility of using the salient pole rotor design in high-speed (Lamghari-Jamal et al., 2006) and extremely high-speed (Fukao et al., 1989) machines. The axially laminated rotor design has a good saliency ratio and performance, but the eddy current losses as a result of the axial lamination are larger (Matsuo and Lipo, 1994). However, the mechanical design is extremely complex for industrial manufacturing, at least for four-pole machines, where the sheets have to be bent and connected with bolts (Chalmers and Musaba, 1998). However, a two-pole axially laminated machine is easier to manufacture because the electrical sheets are straight (Torac, 2001). A two-pole axially laminated structure can also be produced by explosive bonding (Hofmann and Sanders, 1996, Hofmann and Sanders, 2000). The structure becomes very rigid and solid, but the manufacturing process is still complicated. In practice, the transverse laminated rotor design is the best choice for industrial manufacturing, because similar sheets can easily be punched and iron losses in the rotor are reduced compared to the axially laminated structure (Vagati et al., 2000a). Therefore, all the machines studied in this dissertation have the transverse laminated structure.

2.2 Synchronous permanent magnet machines

A rotor of a synchronous permanent magnet machine could be inside, outside, or on the sides of the stator. There are also many other combinations of rotors and stators. The rotor structures inside the stator also have many forms. In particular, the magnets can be arranged in many ways, as shown in Figure 3. For example, Morimoto et al. (1996) compared many configurations of the magnets.

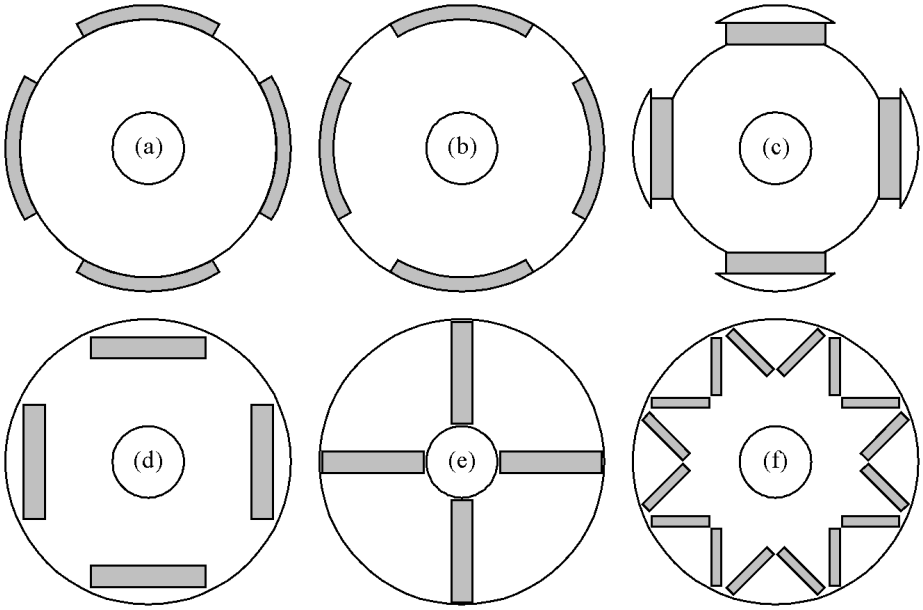

Figure 3: (a) surface-mounted magnets; (b) inset rotor with surface magnets, (c) surface magnets with pole shoes; (d) embedded tangential magnets; (e) embedded radial magnets, and (f) embedded inclined V-magnets.

In one of the most common rotor structures nowadays, the magnets are mounted on the surface of the rotor (a). This structure is simple and easy to manufacture. However, surface magnets are not well protected and it is difficult to keep them still on the rotor surface, especially at high rotational speeds. By insetting magnets into the rotor surface (b) or covering the magnets with pole shoes (c), the magnets are more protected. Continuing this development, the magnets become embedded (d-f). The magnets are better protected inside the rotor than on the surface of the rotor, as discussed by Jahns and Nocker (1989) in (c) and Jahns et al. (1986) in (d). Yamazaki et al. (2009) analyzed and compared eddy current losses in rotors with surface-mounted, inset, and embedded magnets (a, b and d). They showed that the eddy current losses were smallest in the embedded magnet rotor and largest in the inset magnet rotor.

In addition, embedded magnets give an opportunity to increase the flux induced by the rotor by concentrating it. One solution for increasing the rotor flux is to use radial magnets (e). For example, Spooner and Williamson (1996) analyzed and measured a modular multi-pole radial permanent magnet generator. Belmans et al. (1989),

Teixeira et al. (1993), and Binns et al. (1993) studied low pole number rotor structures with deep radial magnets, where the saturation level of the iron is high.

In many embedded magnet solutions the flux leakage should be considered in the design process. For example, Tsai and Tsang (1999) analyzed the flux leakage with embedded tangential magnets (d).

The starting point of the permanent magnet machine design in this dissertation is a rotor where the magnets are of an inclined V-shaped form and the pole shoe is cosine-shaped (Salo et al., 2000). Heikkilä (2002) performed deep analysis of the usage of the V-shaped design with a cosine-shaped pole shoe. The cosine-shaped pole shoe forms the air gap flux sinusoidal distribution and the back EMF is also sinusoidal. However, the air gap flux could also be formed sinusoidally by using guiding holes for concentrating the flux to the middle of the poles, as shown by Kolehmainen (2005). Lee et al. (2003) and Junak and Ombach (2010) optimized the air gap form for minimizing the harmonics of the back EMF. Their optimization process also takes into account the saturation effects.

2.3 Permanent magnet-assisted synchronous reluctance machines

The electrical performance of synchronous reluctance machines (SRMs) can be increased by inserting permanent magnets into the rotor core (Niazi, 2005). These machines are usually called permanent magnet-assisted SRMs (PMASRM) (Bianchi and Bolognani, 2002); see Figure 4(a).

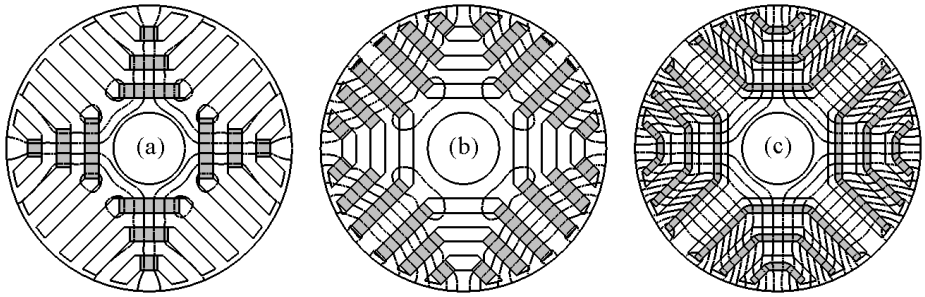

Figure 4: Permanent magnet-assisted synchronous reluctance motor solutions. Flux lines produced by magnets are also shown.

Morimoto et al. (2001) (a) showed that the PMASRM construction increases the efficiency at light loads compared to the SRM construction and uncontrolled generator mode operation in high-speed flux-weakening operation has lower risks compared to PMSMs. They performed comparisons of PMASRMs without magnets and different numbers of magnets in the flux barriers. Therefore, PMASRMs are suitable for wide constant power applications and a wide flux-weakening range (Barcaro et al., 2010) in (a). In addition, Lee et al. (1999) in (b) studied the increase in the inductance ratio as a result of adding magnets to the SRM rotor. They also showed that only a small amount of magnet material is needed to reach a relatively high power density and power factor.

In addition to solid rectangular magnets, Sibande et al. (2004 and 2006) used easily shaped epoxy-bonded magnet material sheets on the outer surfaces of the flux barriers of an SRM (c). Axially laminated SRMs can also be assisted by the magnets, as was done by Soong et al. (1995). The electric properties of a PMASRM are usable for hybrid vehicles, because they have large speed and power ranges, as discussed by Boldea et al. (2004 and 2006) (a).

2.4 Strengthening methods of axially laminated rotor structures

In synchronous permanent magnet and reluctance machines, the rotors are constructed of magnetically separated parts. In the rotating rotors, finding a simple, strong, and magnetically good solution to fix the rotor parts together is always a challenge. If one property is better designed, the other properties are usually not so good any more. In this chapter, existing methods for connecting the rotor parts of synchronous permanent magnet and reluctance machines are introduced and discussed.

2.4.1 Bridges between skeleton and supported part

Conventional method

One of the simplest and most usable methods to create buried magnet and synchronous reluctance machines is to use monolithic rotor sheets, where some iron bridges to the structure are left in the cutting process (see Figures 5(a-c) and 6(a)). The iron bridges then support the structure (Lovelace et al., 2004) but, unfortunately, the supporting bridges cause the electrical properties of the rotor to deteriorate, because the bridges work as paths for the leakage flux (Hwang and Cho, 2001 and Lovelace et al., 2000). Therefore, part of the magnetic field produced by the magnets is lost and more magnetic material is needed. However, the saturation of the bridges reduces the leakage flux in permanent magnet machines.

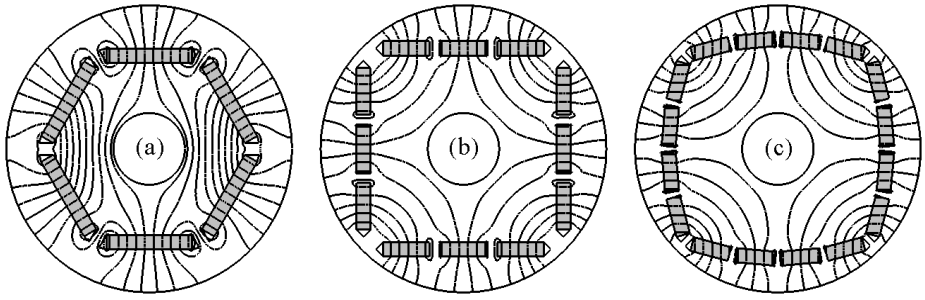

Figure 5: Magnets and supporting bridge configurations of PMM rotors. Flux lines produced by magnets are also shown.

For example, Kamiya (2005) studied how many bridges are needed to reach the desired rotor speed durability and what the effect on the electrical performance is. Jayawant et al. (1995) studied a structure with three bridges per pole and high strength but low electrical performance for the rotor of the magnetic bearings (Figure

5(a)). However, Dutta and Rahman (2008) (b) and Stumberger et al. (2001) (c) used three and four bridges per pole with high leakage flux for widening the constant power speed range of the machine.

The leakage flux paths of SRMs have to be saturated by using more current. Vagati et al. (2000b) studied the impact of cross-saturation. However, as explained in Chapter 2.3, the saturation of SRMs can also be achieved by means of permanent magnets.

Bi-state sheets

One advanced method to reduce the leakage flux through the supporting bridges is to use bi-state soft magnetic material, which can be treated nonmagnetic by heating (El-Refaie et al., 2004; El-Refaie and Jahns, 2005; El-Refaie, 2005). Then thicker and stronger supporting bridges can be used, with good electrical properties. Thicker supporting bridges make it possible to increase the maximum speed of the rotor. However, the bi-state material is more expensive and has much lower permeability in untreated areas than the silicon steel which is commonly used for electrical machines.

2.4.2 Additional supporting devices

Rotor sheets can also be punched into many pieces to reduce the leakage flux between the poles of PM machines and the flux paths of SR machines. Therefore, an extra supporting structure is needed. For example, a typical supporting method (shown in Figure 6) for V-shaped buried magnet pole structures is to support the separate rotor poles with H-shaped bars in the bottoms of the V-shaped poles (b) (Knauf and Vollmerr, 2003). Hershberger (1982) also introduced a structure where the magnets support the rotor poles longitudinally (c). However, this is not a suitable structure for high-speed machines.

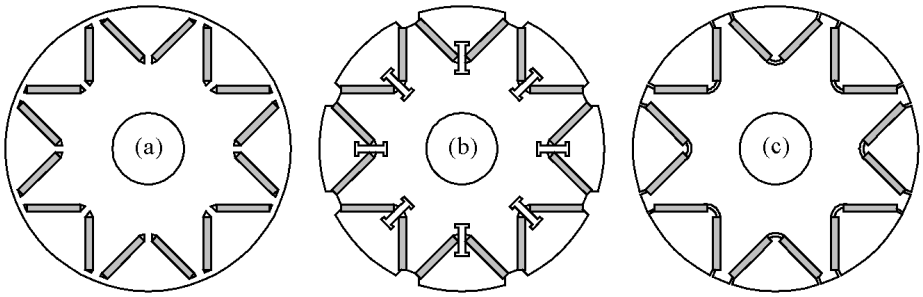

Figure 6: Methods for supporting rotor with V-shaped permanent magnet rotor.

Three-dimensional supporting methods can also be used as additional or as the only means of support of the rotor parts. For example, separated pieces of the rotor structure can be supported with axial bars, which are supported by non-magnetic parts, like strong plates, inserted into the rotor. If many non-magnetic parts are needed in the rotor, the magnetically active part of the rotor becomes shorter. However, three-dimensional supporting structures are often difficult and expensive to construct.

2.4.3 Dovetail magnets

The shape of the magnets is also used for locking the magnet itself structurally to the rotor. Both surface-inset and radial magnets can be locked to the rotor, as shown in Figure 7. For a surface-inset magnet rotor, supporting parts can also be used for increasing the reluctance torque, as shown by Gan et al. (2000a) and Gan et al. (2000b).

However, surface-inset magnets can also be inserted into every second pole, as in (a). This structure is called a consequent rotor structure. Takenaga et al. (2002) proposed the principle and the design of the consequent pole motor. Amemiya (2005) compared the consequent pole PMSM rotor with a conventional surface-mounted PMSM rotor. An uneven magnet pole width ratio for a consequent pole motor could also be considered (Bolognesi et al., 2010).

Consequent pole rotor designs with embedded magnets were introduced by Evans (2008) and Evans (2010). The consequent rotor design could also be called a unipolar design (Nedjar, 2010). The consequent pole rotor gives more opportunities to create dovetail pole structures, as will be shown later.

Radial magnets are easy to lock structurally to the rotor, as shown in Figure 7(c). This method is good for low-speed and high pole number machines (Suh et al., 2006 and Halberg, 2005). However, the method also needs some connection structure to fix the rotor iron. A dovetail-shaped connection method has been proposed to fix the rotor iron parts to the shaft (Halberg, 2005, Meier, 2008, and Marino, 2009) (c).

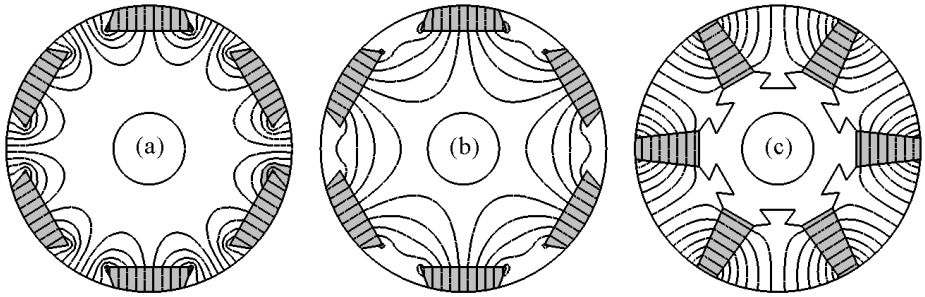

Figure 7: Principles of locking permanent magnets to a rotor.

2.4.4 Dovetail poles

In addition to keeping the permanent magnets structurally locked onto the rotor, the magnets can also be used for blocking some parts of the rotor. V-shaped and radial magnet rotor structures can be blocked together by arranging a retaining hook in the rotor sheets above the top of the magnets and bottom of the separate poles, as shown in Figure 6(c). However, this is not a very strong supporting method because the magnets support the poles longitudinally.

The magnets can hold forces better in their lateral direction, as explained later. One solution proposed earlier was invented by Jacques and Pascal in 2001. The explanation of their solution, shown in Figure 8 (left), is: “The rotor of an electrical machine is made from laminations (4), each lamination having a central annular area

(4e) and four peripheral sectors (4a, 4b, 4c, 4d) which define hourglass-shaped cavities (6). The cavities (6) house laminated pole pieces (7) and two pairs of flux-concentrating permanent magnets (20a, 20b, 21a, 21b) which are secured by the shape of the housing and pole piece." Their second proposed design is shown in Figure 8 (right).

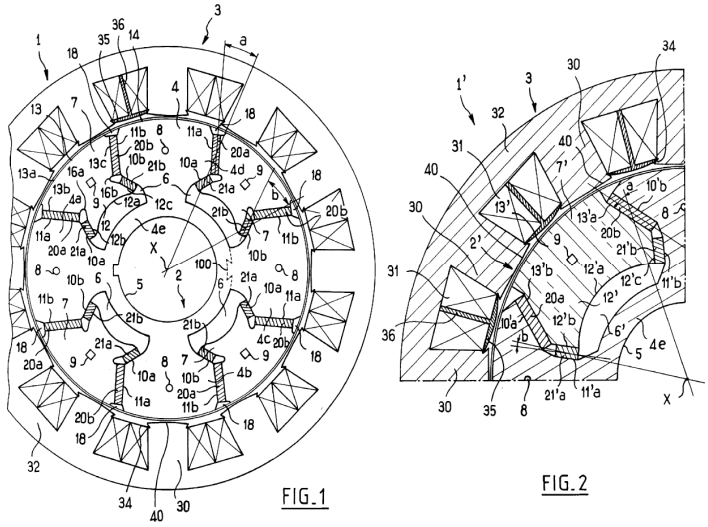

Figure 8: Dovetail solutions of Jacques and Pascal (2001).

More dovetail form-blocked solutions of PMSM poles are studied later in this dissertation. The flux path of the SRM can also be supported with a similar method as will be explained later in the dissertation.

2.5 Applications and usage of PM and SR machines

Just as there are many different machine solutions, there are also many applications for using them (see Table 1). There are four common load types for synchronous machine applications. They are constant torque, quadratic torque, constant power (Morimoto et al., 1996 and 2001), and constant power/torque loads. Typical constant torque applications are conveyors, feeders, screws, and compressors. Centrifugal pumps and fans have quadratic torque versus speed characteristics. However, rollers need constant power. A combination of constant power and torque is needed, for example, for paper machines and electric vehicles (Kamiya, 2005, Dutta and Rahman, 2008 and Sibande et al., 2006).

"Electric traction drives require an ability to operate at constant power over a wide speed range, good overload performance, and high efficiency, especially at light-load operation at higher speeds. These characteristics allow the best utilization of the limited battery capacity and minimization of the size and weight of the motor and drive" (Soong et al. 2002).

Table 1: Common load types, applications, and load curves for PMSM and SRM.

Constant torque	Quadratic torque	Constant power	Constant power/torque
Conveyors Feeders Screws	Centrifugal pumps Fans	Rollers	Paper machine rolls Electric vehicles
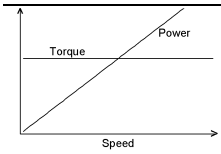	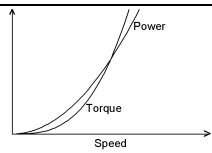	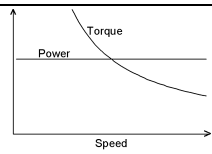	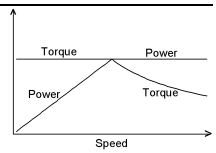

2.6 Conclusion of earlier solutions

Various axially laminated SRM and PMSM solutions were presented earlier. The literature study shows that when the electrical or mechanical rotor properties are improved by changing only the rotor dimensions, the other properties become worse. However, both the electrical and mechanical properties of the rotor could be made better by using some additional supporting devices or more expensive materials. Therefore, there exists a dilemma between the electrical properties, mechanical durability, construction complexity, and material price. It is difficult to make one property better without worsening the other properties. This dissertation concentrates on solving this dilemma by using dovetail rotor structures.

For PMSMs this means that the magnets support their own centrifugal weights and that of the motor pole. Only one earlier study was found, the patent of Jacques and Pascal (2001), where the magnets also support the other rotor parts than the magnets themselves. However, no scientific studies where the magnets also support the other rotor parts were found.

3 Design methods

In this chapter, the principles for designing a dovetail synchronous reluctance machine (SRM) and dovetail permanent magnet synchronous machine (PMSM) are presented. First, the dovetail PMSM and SRM rotor designs are introduced. The design principles of dovetail rotors and stators are considered. The material properties and mechanical analysis methods are presented. Finally, the electromagnetic analyzing principles and methods are shown.

3.1 Introduction to dovetail PMSM and SRM rotors

In the dovetail design, parts of a rotor are structurally blocked by the form of other parts of the rotor. In the dovetail PMSM rotor, poles are form-blocked with the help of the magnets. However, the magnets can also be used to support the SRM rotor structures. The machine would then be a PM-assisted SRM. A non-magnetic filler material could be used in the supporting parts. Then the machine is a dovetail SRM. The principles of the dovetail PMSM and SRM designs considered here are shown in Figure 9. The dovetail PMSMs designed in this work (in P2, P3, P4, P5, P7 and P8) are also consequent pole machines, because consequent pole PMSM rotor design gives more design opportunities, as shown in P1.

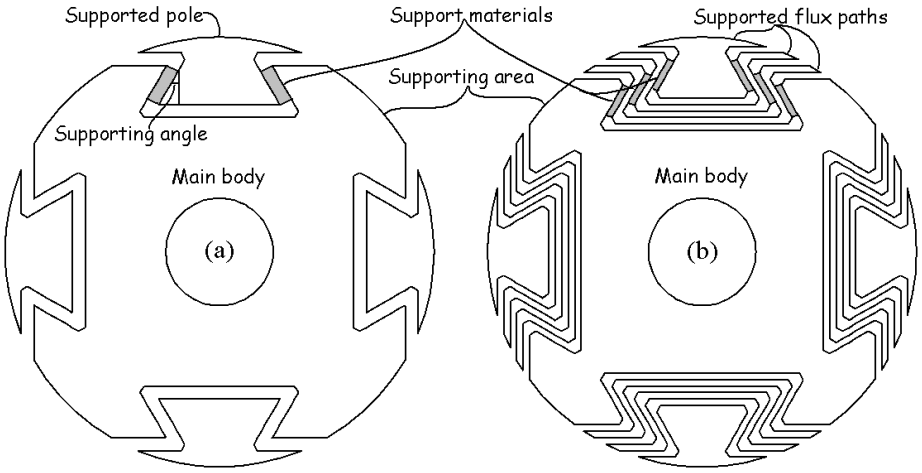

Figure 9: Principles of dovetail PM (a) and SR (b) rotor structures.

3.2 Design principles of dovetail rotors

The design methods of dovetail rotors differ from the methods for the original designs, where the rotor poles are fixed to the rotor main body only by the supporting bridges. If the thickness of the supporting bridges in the original designs is increased, the strength and the leakage flux increase and the electrical properties worsen. However, the increase in the dovetail design strength does not necessary lead to the worsening of the electrical properties. Rather, they have optimum structures near each other, as shown in P4.

Although the mechanical properties could be analyzed only for the rotor, the stator should somehow be taken into account when seeking the best electrical properties of the rotor. In this dissertation, the prototype rotors are electrically designed for specified real stators using the following method. First, the rotor dimensions are intuitively chosen on the basis of earlier knowledge. Then the mechanical properties of the rotor and electrical properties of the whole machine are analyzed. After the analyses, the rotor dimensions are intuitively chosen again until the best solution is found. This process follows the smallest loops in the design flow chart in Figure 10.

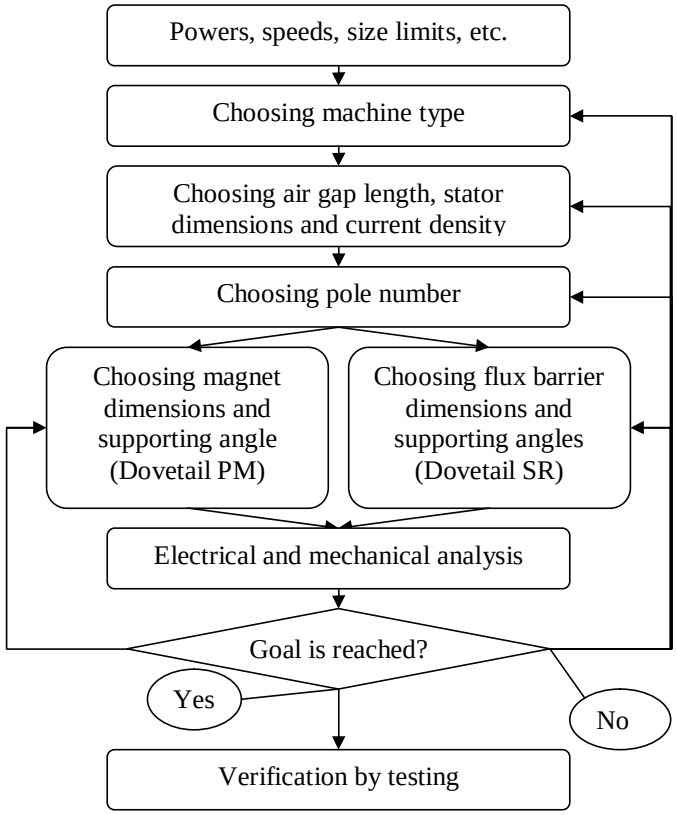

Figure 10: Flow chart of design process of dovetail PMSM and SRM.

In this dissertation, a design method to find the best rotor solution without taking the stator properties into consideration is also proposed. In the method, the stator is simplified so that there are no stator slots and no winding. In addition to finding the best rotor dimensions, this also gives a better opportunity to study the effect of the pole number on the mechanical and electrical properties. The detailed study for a PMSM is shown in P4. One of the main results is that by increasing the pole number, the maximum speed can be increased, but at the same time, the electrical properties are reduced. (However, for a higher pole number, a higher supply frequency is also needed, which increases the iron losses of the whole machine.) This design process

follows the second smallest loop in the design flow chart in Figure 10. The other important result of this study (in P4) is that the best supporting angles are shown to be the same angles as the rotor surface has in the middle of the supporting poles. In addition, if only the width of the supporting magnets is increased, the mass of magnetic material increases and the main body saturates between the supported poles. Therefore, the supporting magnets have an electrically optimal length. However, in P4 it is also shown that it is enough to find the best electrical width of the supporting magnets in order also to find almost the maximal mechanical strength of the rotor. So it is sometimes enough to find the best electrical solution in order to find the best mechanical solution in dovetail PMSM designs.

3.3 Overall design procedure

In this dissertation, dovetail designs are used to replace existing rotors with new designs where the mechanical and/or electrical properties are better. Therefore, the design procedure used is first to find a corresponding machine with the old rotor structure and to modify it to the dovetail structure. However, if there are no existing structures, a totally new design should be created. It may be possible that the new and better design will have a different stator winding and pole number.

In order to finding the optimal design of the machine, the strength of the rotor should be taken into account during the optimization process. The usual way is to find the structure which satisfies the mechanical constraints, then perform the electrical analysis and then repeat this process until the optimal electrical properties with satisfying mechanical properties are found. For example, Kamiya (2005) searched for the minimum number of supporting bridges between the magnets and compared the leakage flux. Lovelace et al. (2004) used mechanical finite element analysis for analyzing stresses, especially in the tangential and radial supporting bridges in a buried PMSM rotor. The influence of mechanical strength on the electrical properties is also compared. In high-speed machines, thermal behavior and vibration analysis could also be important, as discussed in the work of Zaim (2009) for their innovative salient pole rotor SRM and in the work of Castagnini et al. (2002) for a very high-speed and high-power PMSM. However, all the machines studied in this dissertation have natural frequencies that are clearly above the desired speeds and the temperature rise was no problem. In addition, Pyrhönen et al. (2008) presented a good overview of the design of rotating electrical machines.

The overall design process for the dovetail machines considered in this work is shown in Figure 10. The starting point of the design of all electrical machines is first to find the right dimensions, machine type, pole number etc. This is usually based on the experience of the designer. However, many earlier designs may exist which can be used as the starting point of the design process. After the initial guess has been chosen, the electrical and mechanical analyses have to be performed to see if the design is good enough for its planned usage.

In this dissertation, all the stators of the dovetail PMSMs were originally defined for V-shaped PMSMs and all the stators of the dovetail SRMs for cage induction machines. The validity of the dovetail designs is modeled by using the two-dimensional electromagnetic and mechanical finite element methods (FEM) (these

methods are presented later). Finally, the modeled results should be verified by testing.

3.4 Material properties

When performing the electrical and mechanical analyses, the material properties should be known. The materials used in the dovetail permanent magnet rotor are the magnets, the electrical steel sheets, and the material between the magnets (usually glue). In the dovetail synchronous reluctance rotors, only glue or non-magnetic steel bars between the rotor parts made of electrical steel sheets have been used.

3.4.1 Permanent magnet material

When designing permanent magnet machines, it is important to know the magnetic properties of the permanent magnets. However, the magnets should also be strong enough to support at least their own weight against the centrifugal and magnetic forces. In the dovetail designs, the magnets are also used for supporting the other rotor parts, such as rotor poles. Therefore, more attention should be paid to the strength properties of the magnets. The compressive strength of the magnets is critical to the whole rotor strength in the dovetail machine solutions considered here.

Neodym-Iron-Boron (Nd-Fe-B) is nowadays the most powerful magnet material in electrical machine technology, because it can create the largest magnetic flux. Therefore, it is also used in the dovetail PMSMs considered in this dissertation. Mechanically, the Nd-Fe-B material is quite strong but it might be quite brittle. There is very little likelihood that it will deform before fracture. Brittleness is caused by the manufacturing process. “Nd-Fe-B magnets are produced powder metallurgically by sintering. The process starts from the hydrogen decrepitation and fine milling of the raw material. The resulting powder is then compressed into the desired shape and at the same time its particles are aligned using a magnetic field. The compressed blocks are sintered and machined into the final dimensions before coating and magnetizing” (Neorem, 2010).

In the dovetail design, the magnets are pressed between the supporting and the supported parts mainly by the centrifugal force. The largest surfaces of the magnets take the compressive force. If the force has some deviations, because of deformation or local deviations of the supporting or supported rotor parts, the flexural stress could crack the magnets. Because of the flat shape of the magnets, the magnets are expected to fracture into pieces which still support the structure as well as non-fractured magnets. There is also glue between the magnets and the compressive parts. The glue smooths local force peaks and the danger of fractures decreases. Thin metal sheets can also be used for smoothing, as was done in P7.

Li et al. (2005) showed experimentally that when rare earth magnets are bent (also Nd2Fe14B) the crack always starts in the tensile area and propagates through the whole magnet. In the fractures that were studied, no section shrink, no fiber region, and no shear lip were found. The fracture of Nd2Fe14B is typically brittle. Li et al. showed that the fracture mechanism of an Nd2Fe14B magnet mainly appears to be intergranular fracture. In addition, Horton et al. (1996) saw in studies of three commercial Nd2Fe14B magnets that no orientation differences were observed

between the magnets fractured parallel or normal to the grain direction. However, all the magnets used in this dissertation are magnetized in the perpendicular direction and the grains are oriented in the same direction (Neorem, 2010). Therefore, the magnets used here have a tendency to crack directly in the perpendicular direction. In the dovetail structure, the magnets are then first expected to crack into pieces, which have practically the same strength as the original magnets against the pressure force. However, no cracks were detected in any prototypes tested in this dissertation.

To demonstrate the crack directions, the author made a small study of Nd-Fe-B magnets (Neorem, 2010), where thin magnets were cracked with a plastic hammer on a smooth table. The thickness, width, and length of the magnets that were tested were 4.6 mm, 45 mm, and 50 mm, respectively. The results, shown in Figure 11, support the assumption that the cracks appear nearly in the perpendicular direction of the flat magnet.

Figure 11: Pieces of two hammered Nd-Fe-B magnets.

Failures of brittle materials can also be caused by a dynamic load, particularly by an impact load. Li et al. (2009) studied the impact stability and strength properties of sintered Nd-Fe-B magnets. They also showed that Nd-Fe-B magnets may have a maximum bending strength of up to 397 MPa with the right rates of materials without any sacrifice of their magnetic properties. However, they stated that the average bending strength of sintered Nd-Fe-B magnets is around 280-330 MPa. The manufacturing process of the magnets clearly affects the strength.

For the Nd-Fe-B magnet material used in this dissertation, the typical tensile and flexural strength are proposed to be 70 MPa and 240 MPa, respectively. For greater safety, the maximum permitted stress of the magnets is chosen to be a tensile strength of 70 MPa with a safety factor of 1.5 in spite of the higher flexural strength. However, in the studies of this dissertation, the strength of the magnets was not critical for the strength of the dovetail rotors. No fractures of the magnets were seen in any machines tested for this dissertation.

3.4.2 Electrical steel

The mechanical properties of electrical steel are totally different from those of magnets. If there are local stress peaks which are under tensile strength in electrical steel, it just yields locally and the stress is reduced. However, after many periods of local yielding the material might crack. But the Nd-Fe-B magnet material just cracks at the beginning of the load, if it cracks at all. For the M400-50 electrical sheet material (Surahammars Bruk, 2010), which is typically used for the machine types analyzed in this dissertation, the yield and tensile strength are 300 MPa and 400 MPa and the Young's modulus is 205 GPa. However, stronger electrical sheet materials where the tensile strength is up to 500 MPa could also have been used (but these have lower magnetic conductivity).

3.4.3 Magnetic properties of electrical steel

The magnetic properties of electrical steel play an important role in electrical machines. As the magnets can create a flux density around 1.15 T, electrical steel can be used to increase the flux density to over 2 T. However, the maximum flux density cannot be very much over 2 T, because of the magnetic saturation of the electrical steel used. The saturation curves for M400-50A electrical steel can be found on the web pages of Surahammars Bruk (2010).

3.4.4 Filler glue

As the centrifugal force pulls the supported parts of the rotor outwards, the supporting parts and the epoxy glue between the parts lock the pole firmly in its place and prevent it from moving. The compressive force is the dominant force in the filler material, although it also prevents the parts from sliding. Anti-adhesive filler materials can also be used.

Although the epoxy material is rather soft compared to electrical steel, the epoxy layers tolerate compressive stress well (up to 15-21 MPa). At the same time, the large contact area between the pole wedge and the epoxy renders the compressive stress under the yield strength. The epoxy material also reduces the maximum stress peaks in magnetic materials caused, for example, by clumps of material.

3.4.5 Non-magnetic steel

Non-magnetic steel sheets can also be used between the supporting magnets and supported and supporting rotor parts to smooth the stress peaks. Their mechanical properties are near to those of electrical steel. Non-magnetic steel bars are also used to support the SRM rotor structure, as will be shown later.

3.4.6 Magnetic properties of Nd-Fe-B

The magnet material mostly used in this dissertation, Neorem 495a, is sintered Nd-Fe-B (Neorem, 2010). The remanence and intrinsic coercivity of Neorem 495a magnet material at 20 ºC are 1.15 T and 2440 kA/m. The thermal dependence of remanence and intrinsic coercivity are remarkable and should be taken into account. The thermal remanence factor used is $1 + \alpha \cdot (T - 20^{\circ}\mathrm{C})$, where $\alpha = -0.0011$.

3.5 Mechanical analysis of rotor

In this dissertation, the strength of the rotors is estimated by using a two-dimensional finite element method (FEM) with the stress-strain model (Comsol, 2010). In the rotor of an electrical machine, the forces that exist are caused by many factors. The electromagnetic forces are the most important forces in low-speed and high-torque applications. The centrifugal force is the largest force in higher-speed applications. The forces produced by heat gradients in the rotor could be important, especially when the loading state is changing rapidly. However, in this dissertation only the centrifugal forces are studied, because they are seen as being the critical forces in our cases in the multi-physical FE models created by the author (Comsol, 2010).

In all the dovetail designs, critical regions for strength against the centrifugal force are near the supporting material between the supporting and the supported parts. In addition, if there are some extra bridges between the parts, these have to be taken into account in the strength considerations.

In order to gain an understanding of the problems of defining the strength, several models and rotor constructions are considered in this chapter.

3.5.1 Strength of PM rotors with glued magnets

The basic method used to install the magnets into a PM rotor is gluing. The analyzing model consists of three materials, i.e. the electrical sheets, magnets, and glue. In the original V-shaped magnet rotor, only the bridges between the poles support the structure and the magnets are only the weight in the calculations. In the models of the V-shaped designs, the glue between the magnets and the main body of the rotor does not need to be modeled. The maximum speed can just be defined from the maximum von Mises stresses and safety factor with the equation:

$$n_{\max} = n_{\text{model}} \cdot \sqrt{\sigma_{\text{yield}} / (\sigma_{\text{modeled}} \cdot \eta)}, \quad (1)$$

where $n_{\max}$, n_{model}, η, σ_{yield}, and σ_{modeled} are the maximum speed, speed used in the model, factor of safety, yield strength, and modeled critical stress.

However, in the dovetail PM rotor design, the magnets are used to support the rotor structure and the glue to smooth the stress peaks between the supporting and supported parts. Glue is modeled as real layers between the parts with a thickness of 0.35 mm. The maximum speed of the pure dovetail design (P3 and Figure (25(a) in Chapter 5)) is easy to define from the maximum von Mises stresses. However, the bridges make defining the strength more complicated. The maximum stresses of the dovetail structure might be higher in the structures where the bridges are also used. For example, for the dovetail machine in P2 (Figure (25(b) in Chapter 5), frame size 250, bridges between the poles), the defined maximum speed with bridges between the poles is 0.79 times lower than without the bridges if the strength is defined directly from the maximum von Mises stresses. In this case, the maximum speed is defined without the bridges even though the real rotor with the bridges is stronger.

To get a deeper view, the dovetail rotor structure presented in P5 is studied here. This rotor structure has only tangential bridges between the poles. In this chapter, the study in P5 is also continued for a rotor where the tangential bridges were cut away.

The stress distributions of the original V-shaped design and the dovetail design with the bridges and the cut bridges are shown in Figure 12. The largest von Mises stresses of each structure are marked as x. In the V-shaped rotor, the largest and mechanically most critical stress, 97 MPa, is localized in the radial bridges. In the inseparable dovetail rotor, the largest and most mechanically critical stress, 119 MPa, is localized in the tangential bridges. If the bridges are cut away, the maximum stresses of the structure remain at the same level. The maximum stress, 119 MPa, is then located in the main body of the rotor above the corner of the supporting magnets. The maximum stress is assumed to be the critical stress in all the cases.

To validate the strength calculations of the motor presented in P5, six no-load periods from 6000 1/min to 10,000 1/min and a load condition at 9000 1/min for half an hour were run for the rotor where the tangential bridges had been cut away. For the assumed yield strength of 305 MPa the machine is expected to yield at the speed of 9526 1/min (when the safety factor is one). However, no implications of deformation were seen during the tests in the visual study after the tests. Although the maximum stresses of the dovetail design with and without the bridges are close, the bridges make the structure practically stronger than its strength as defined from the maximum stresses.

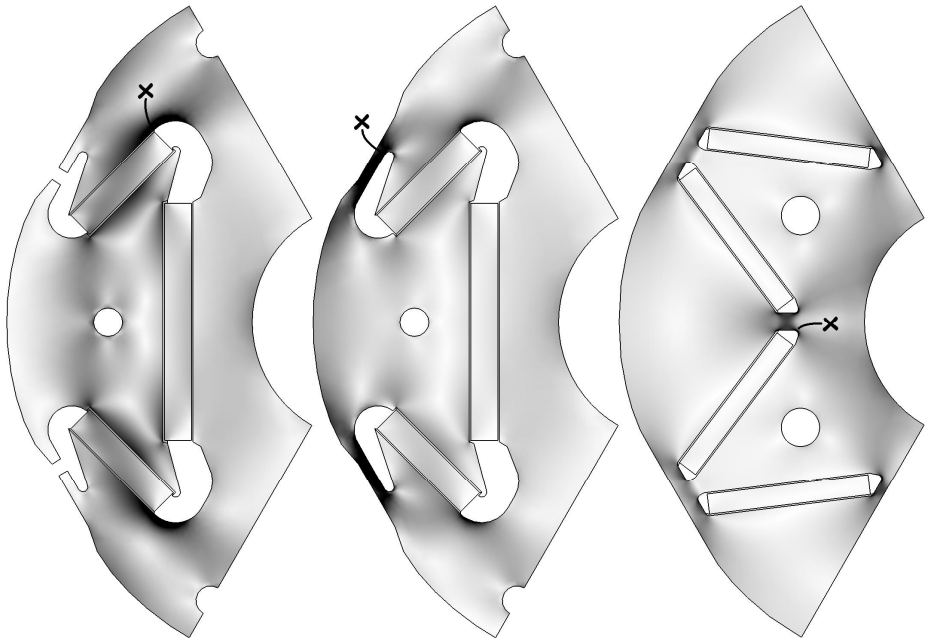

Figure 12: Von Mises stress in the rotors with dovetail and V-shaped designs at a speed of 6000 1/min. Light areas have the lightest stresses starting from 0 MPa and black areas have stresses over 60 MPa. The maximum stress points are marked as x.

3.5.2 Strength of PM rotors without glue

In the PMSM rotor in P7 and P8, the magnets are installed in such a way that there are non-magnetic steel sheets between the magnets and electrical steel stack. In this case, the sliding effect should be taken into account. The effect of sliding can be seen in Figure 13, where the modeled displacements are shown as arrows. When the supporting magnets are sliding, the main stress is a compressive one and it is in the supporting parts. If the supporting parts are glued or somehow stuck, there are also remarkable shear stresses in the supporting parts. This effect can be critical for the supporting magnets. However, if there is no sliding effect, the other critical parts may have lower stresses.

The sliding effect may also grind the surfaces between the parts because of load and speed changes and because of vibration. Therefore it is good to prevent the sliding by gluing.

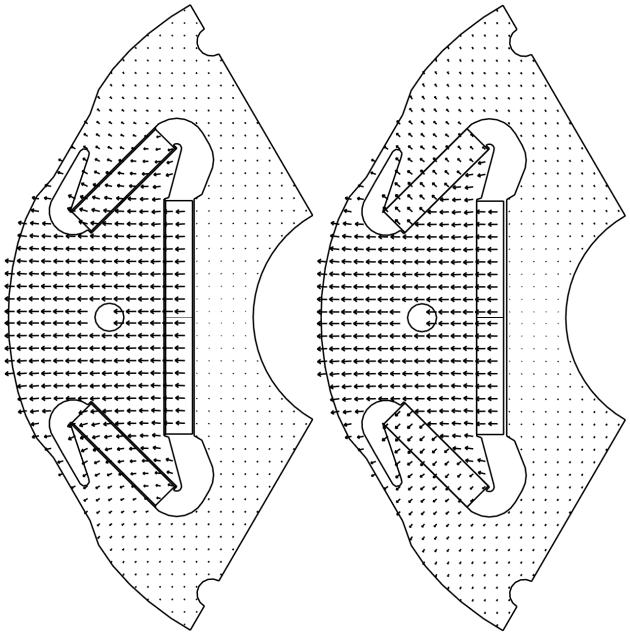

Figure 13: One third of a PMSM where the pole is supported though magnets. The modeled displacement as arrows for the non-sliding (glued) (left) and sliding (right) magnets are shown.

3.5.3 Strength of glued dovetail SRM rotor.

In the glued dovetail SRM rotor (presented in P6), the flux barriers are constructed in such a way that the pressuring durability of the glue between the flux paths prevents them from moving. Naturally, an inseparable mechanical analyzing model can be used. The difficulty of defining the model is to choose the area to be filled with glue. If the glue is only in the areas form-blocking the flux paths, the flux paths tends to deform (as can be seen when only supporting bars are used). This can be seen on the right-hand side of Figure 14. If the glued area is increased as on the left-hand side of Figure 14, more realistic results and better speed durability of the rotor can be achieved.

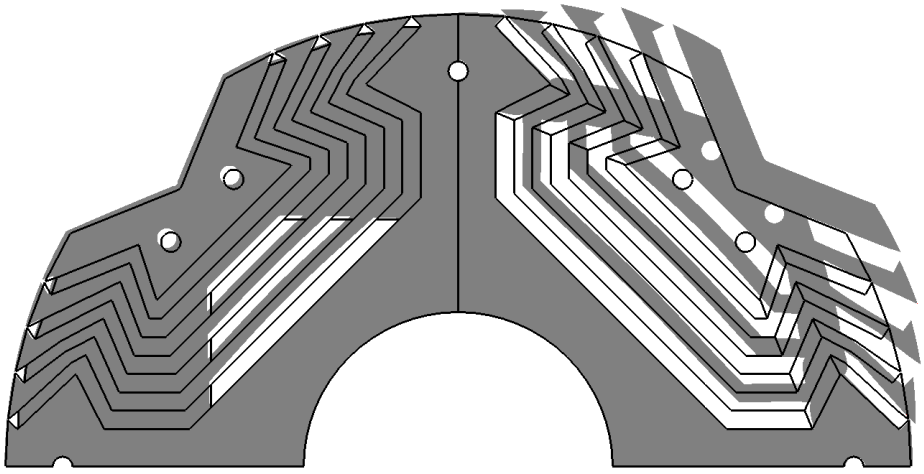

Figure 14: Modeled deformations of dovetail SRM with different amounts of supporting glue in two poles. Deformation scale in the both sides is the same.

3.5.4 Strength of SRM rotors with supporting bars

An SRM where the flux paths are supported by nonmagnetic steel bars is quite complicated to analyze. It is difficult to know how the supported parts and the supporting bars slide relative to each other. The supporting bars which can and cannot slide and are also glued are modeled and compared in Table 2. The maximum stress and the maximum deformation in the air gap are the most critical for the reliability of this SRM. The critical stress points are in the tangential bridges of the outer flux paths and in the electrical steel corners under the innermost supporting bars (see "x" on the right-hand side of Figure 15). The critical deformation points are in the outermost surface of the outermost flux path (see "x" on the left-hand side of Figure 15). If the bars are stuck to the electrical steel, an inseparable and non-sliding mechanical model could be used. Although the maximum stresses are located at the supporting corners, the critical stresses are in the tangential bridges between the two outermost flux paths. The worst case is that the bars slide fully and then the maximum stress increases remarkably.

Table 2: Comparisons of strength models of the bar-supported dovetail SRM.

	Maximum stress (MPa)	Maximum deformation (μm)	Air gap decrease (μm)
Inseparable	679 (Corner), 263 (Bridge)	88 (Path)	60
Inseparable, elastic	374 (Corner), 283 (Bridge)	89 (Path)	60
Sliding bars	1110 (Bridge)	470 (Path)	285
Sliding bars, elastic	528 (Bridge)	510 (Path)	311
Fully glued bars	528 (Bridge)	146 (Path)	92
Partly glued bars	607 (Bridge)	193 (Path)	127

In the prototype motor, the air gap at the beginning of the test was 0.6 mm. During rated load tests at a speed of 4500 1/min and power of 120 kW, the machine was broken when the end winding temperature had risen by 76 K. The rotor had become deformed and touched the stator. The rest of the rotor had no deformations after the tests. In conclusion, the rise in temperature caused the rotor to become deformed during the load test and this damage could have been avoided with a larger air gap.

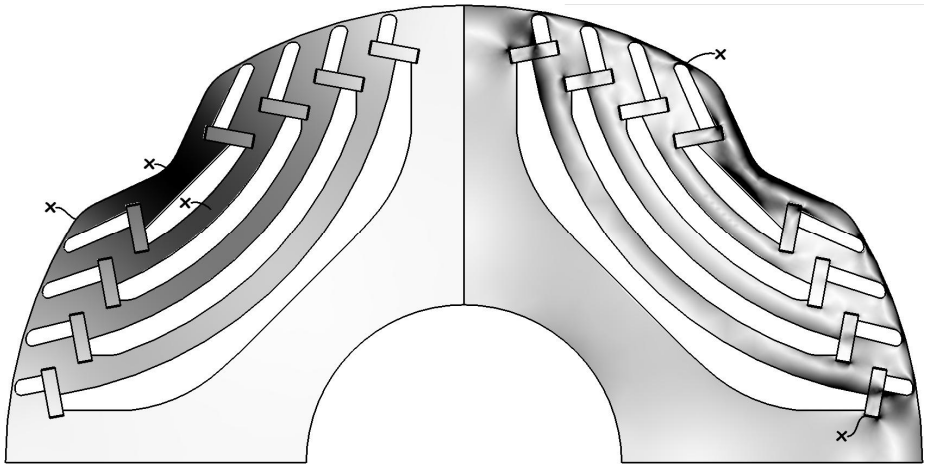

Figure 15: Two quarters of a SRM machine where the pole is supported through nonmagnetic steel bars. Left-hand side: the largest deformation is in black and the sites of the maximum deformations are marked by an "x". Right-hand side: the largest von Mises stresses are in black and the sites of the maximum stresses are marked by "x".

3.6 Electromagnetic analysis of machine

The electromagnetic analyses in this dissertation are performed by using two-dimensional static and time-stepping finite element analysis (FEA) (Arkkio, 1987 and Flux software, 2010). The ways in which electromagnetic FEA is used in this dissertation are presented in this section.

3.6.1 Static finite element analysis

The simplest analysis performed in this dissertation (P4) is a static magnetic FEA of permanent magnet machines without the stator winding. There, the total air gap magnetic flux is calculated for different setups of rotor magnets for finding information about the goodness of the rotor.

Tseng and Wee (1999) used static magnetic FEM for a flux distribution study and simple core loss and induced voltage estimations. Parsa and Hao (2008) also took stator currents into account when studying the load states and torque pulsation of an interior PMSM.

The optimization process is fast when static analysis is used. For example, Ouyang et al. (2006) optimized a permanent magnet machine by using a static back EMF waveform to minimize its time harmonic distortion (THD) and maximize the torque and efficiency. However, definitions of the rotor losses and the other higher-frequency iron losses are lacking in the efficiency calculations of the static FEA. Therefore, static FEM may give misleading results and so the optimal construction is not found.

Static FEA is also used in this dissertation for initial solutions for time-stepping FEA.

3.6.2 Time-stepping finite element analysis

Time-stepping FEA has to be performed to confirm a good motor design, especially when new rotor structures or stator slot numbers are used. For synchronous machines, it is important to see if the torque ripple is at an acceptable level. For example, Bomela and Kamper (1999 and 2002) studied the torque ripple of an SRM using the time-stepping FEA supplied by the current, and estimated the effect of chording with an analytical method.

To get a more realistic view of currents, the machines should be supplied with the voltage supply and right winding connections. Arkkio (1987) created a method and a tool for performing time-stepping FEA that also used voltage sources. This is also important for the studies of the right load angles in Section 4.2.

In this dissertation, the current, the efficiency, and the power factor are defined by the time-stepping FEM and voltage source.

In the efficiency calculations, the stator winding losses are estimated from the current and winding resistance at the assumed temperature. The friction losses are estimated from the existing measurements. The iron losses are calculated from the equation

$$P_{\mathrm{TOT}} = k_{\mathrm{h}} B_{\mathrm{m}}^2 f + \frac{1}{T}\int_0^T \left[\sigma \frac{d^2}{12} \left(\frac{dB}{dt}(t) \right)^2 + k_{\mathrm{e}} \left(\frac{dB}{dt}(t) \right)^{3/2} \right] dt, \quad (2)$$

where B_{m} is the maximum flux density in the element concerned, f is the frequency, σ is the conductivity, d is the lamination thickness, k_{h} is the coefficient of hysteresis loss and k_{e} is the coefficient of excess loss (Flux, 2010). An iron loss equation where the hysteresis and eddy current losses are calculated from the time harmonics of the flux density is also used (Arkkio, 1987 and Arkkio and Niemenmaa, 1992).

However, these equations usually give lower losses than they are in reality. Some of the main reasons are that the effect of hysteresis for the flux density was not taken into account (Saitz, 2001) and the rotational effects were disregarded (Moses, 1990).

3.6.3 Demagnetization analysis

The dovetail design makes it possible to increase the demagnetization resistance by means of the embedded mixed-grade magnets (see P7 and P8) because of the magnets are in two different positions relative to the air gap. Earlier, Ruoho and Arkkio (2007) introduced the idea of a mixed-grade design for a rotor with surface magnets. In addition, Ruoho et al. (2007) and Ruoho and Arkkio (2008) discussed the demagnetization models and partial demagnetization of the permanent magnets.

3.6.4 Three-dimensional finite element analysis

Although radial flux machines can be modeled well with two-dimensional (2D) FEM, the three-dimensional (3D) effects may be remarkable. For example, the leakage flux in the ends of the permanent magnet rotors could reduce the air gap flux remarkably, as shown by Henneberg et al. (1993). Additionally, the eddy currents in rotor magnets are a three-dimensional problem and one that it is necessary to estimate with time-stepping 3D FEM (Ruoho et al., 2008). Ruoho et al. (2009) also compared the three-dimensional results with existing analytical eddy current models used within the 2D FEA of a PMSM.

3.6.5 Rotor analysis method: Force analysis in stator coordinates

In all the FEA in this dissertation, the virtual work method is used to compute the total air gap torque (Coulomb, 1983). The alternative is to use Maxwell's stress tensor method (Belahcen, 2004). Although the virtual work method is more accurate for defining the torque of an electrical machine, the components of Maxwell's stress tensor are useful for investigations of the force generation.

Zhu et al. (2007) studied the local radial and tangential force density components as a function of the air gap angle in their static solutions. The effect of the stator slots is clearly seen in the local force distribution in the air gap.

The tangential force components in stator coordinates could be used for noise and vibration analysis. For example, Belahcen (2004) provides an excellent overview of local force definitions for studying magnetostriction and magnetoelastic coupling.

However, no studies where the local tangential force components are computed in the stator coordinates as a function of the rotor angle or time for analyzing rotor properties have been found.

In this dissertation (in P2), the local tangential components are computed above a stator slot as a function of time. Then the effect of stator slots is neglected and the effect of the rotor design on the torque production can be seen. For example, the asymmetric torque distribution of the dovetail consequent pole rotor can be seen.

The torque per axial length is obtained from the Maxwell stress formula

$$T_{\mathrm{e}} = \frac{1}{\mu_0} r^2 \int_0^{2\pi} B_r B_\varphi d\varphi, \tag{3}$$

where $B_r = B_r(r,\varphi)$ and $B_\varphi = B_\varphi(r,\varphi)$ are the r- and φ-components of the flux density. The local tangential force density is defined as

$$f_{\tan} = \frac{1}{\mu_0} B_r B_\varphi. \tag{4}$$

To analyze the tangential force distribution in the air gap, the normalized local tangential force density is written as

$$f_{\tan}^{\ \mathrm{normalized}} = \frac{f_{\tan}}{\int_0^T f_{\tan}\, dt} = \frac{B_r B_\varphi}{\int_0^T B_r B_\varphi dt}, \tag{5}$$

where T is the time for one electric period. This equation makes it possible to analyze the torque distribution in the air gap without the direct effect of the stator slots. However, the torque could not be defined exactly in the middle of the air gap but it gives an excellent tool for designing the surface structures of rotors.

Figure 16 presents the normalized local torque from Equation (5) at one air gap point of the V-pole and the dovetail consequent pole designs between two stator slots as a function of time. In the dovetail design, there is one sharper torque density peak. However, the average torque density of the two dovetail poles is near to the torque density of the V-shaped design. Going further, despite the sharper stress distribution in every second pole of the dovetail design, the resultant torque oscillation is slightly smaller, as shown in P2. This could be expected from the quite smooth average torque between the dovetail poles. The skewing, which is not taken into account in the simulations but is sometimes present in actual machines, could also diminish the difference.

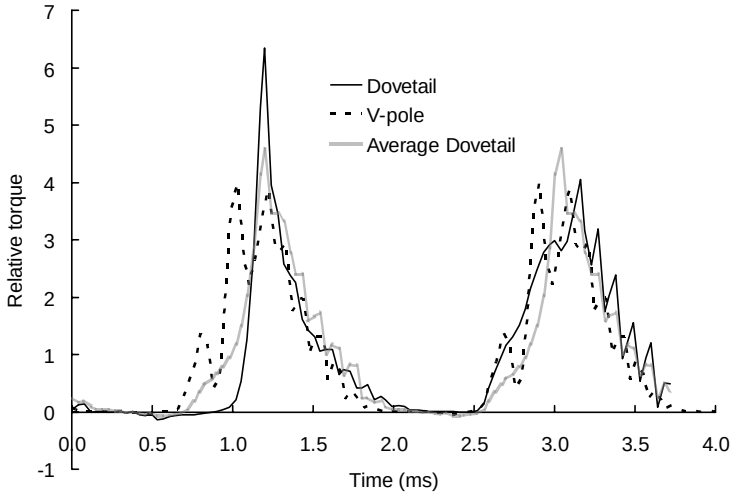

Figure 16: Time distributions of normalized local torque density in air gap of V-shaped and dovetail designs (in P2) at rated load and speed as a function of time.

4 Definition methods

The electrical validity of an electrical machine is mainly proven if the critical temperature rises are below their limits at the desired powers and speeds. However, a larger maximum power and greater speed should also be able to be reached without problems for a short time or making sure that there is no danger of failures such as dropping out of synchronism or balance. See, for example, the test results of a very high-speed PMSM by Castagnini and Leone (2002).

For comparing different machines, studies of temperature differences are very useful. These indicate differences in total losses and loss distribution. However, the loss distribution is difficult to measure accurately. By using values that are easy to measure and comparing them to modeled ones, more accurate estimations of the loss distribution and the electrical properties could be reached.

In this chapter, the test methods used in this dissertation are introduced. In addition, the load angle definition method is introduced. It is used for validation of the calculation models in this dissertation.

4.1 Test methods

4.1.1 Basic tests

This section introduces the test methods which are commonly used for PMSMs and SRMs and also used for the prototypes introduced in this dissertation.

The first test performed on all the prototypes is the no-load test. The no-load test shows whether the durability and the balance of the rotor satisfy the conditions in such a way that the vibration level stays below a predefined maximum level and the same during the test. The no-load current also indicates that the electrical properties are as expected.

The open circuit test shows whether the rotor of a PMSM is electrically as designed. It also shows whether the magnets are installed properly, the rotor is in the middle of the stator, and the air gap is as designed.

Naturally, the load test is the most important test for defining the validity of an electrical machine. The test arrangement principle used in this dissertation is shown in Figure 17. All the load tests presented in this dissertation were performed using DC machines for loading. A gearbox is also used for the machines with rotating speeds over 3000 1/min. Several frequency converters belonging to the ACS frequency converter series (ACS, 2010) are used during the tests. The efficiencies of machines are determined by an input-output method, where the measured mechanical output power is compared to the measured electrical input power of the motor. See, for comparison, the efficiency measurements of synchronous reluctance and induction motors by Haataja et al. (2002) and efficiency measurements of PMSM by Thelin and Nee (2000).

However, the torque transducer used in the torque measurements typically has an accuracy of 1%. It is enough for defining the output power, but for efficiency

definition, it is not accurate enough. Therefore, attempts have to be made to define total losses more accurately with some other method.

For air-cooled machines, one can define the total losses from the rise in the cooling air temperature and total air flow, but this is effortful to install, especially for large machines. For example, Szabados and Mihalcea (2002) used the calorimetric method for defining the losses of a 7.5-kW induction machine. Cao et al. (2009a) and Cao et al. (2009b) introduced calorimeter loss measurements for 300-kW and 30-kW electrical machines. The loss accuracies of these pieces of equipment are from 0.2% to 0.5%. For water-cooled machines, it is easier to define the losses by measuring the rise in the temperature and flow rate of the cooling water. However, some losses in water-cooled machines also move directly into the air.

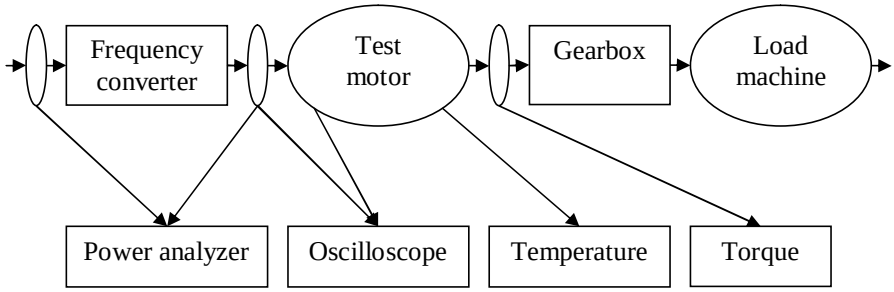

Figure 17: Widest test arrangement used in this dissertation.

Commonly, the total losses are estimated by defining the losses separately. The resistance losses of the stator winding are easy to estimate by measuring the direct current resistance of the winding and the stator current. Therefore, the stator winding losses can be estimated quite accurately. However, the eddy current and circulating current losses in a random-wound stator winding are not taken into account. In some cases these might be remarkable.

The friction losses of SRMs can be measured by letting the machine decelerate freely and measuring the speed deceleration. The friction losses as a function of the deceleration speed are

$$P_{\text{friction}} = -J\omega\frac{\partial\omega}{\partial t} \tag{5}$$

This is easy to use for an SRM, but measuring the friction losses of a PMSM in this way will also include iron losses because of the magnets. However, these losses can still be used for estimating the level of the friction losses and iron losses. It is sometimes assumed that the iron losses are also on the same level in load states, although the iron losses are greater in reality. However, it can be used for checking the loss model in the FEA.

Another method for defining the friction losses of an SRM is reducing the voltage without the loading machine and measuring the input power as a function of the voltage. The friction losses are then extrapolated from the power at zero voltage. The no-load iron losses can also be defined from this experiment.

Temperature rise tests are used to define the maximum power in continuous usage. The temperature rise of the winding and maximum temperature of the machine usually define the load capability of the machine. Critical parts for the temperature rise are the stator winding insulations, permanent magnets (P7 and P8), and sometimes the glue in the rotor (P6). During temperature rise tests, the critical temperatures of the machine are recorded. The machine runs until all the measured temperatures are stabilized and change by less than 2K per hour (IEC 60034-1). After the motor has been stopped, the temperature rise of the stator winding is determined using the resistance measurement. In the basic tests, the temperature rises are determined for the winding, end windings, and hottest assumed place in the frame. However, the rises in the rotor temperature are also measured in most studies in this dissertation. The rotor temperature measurements are performed with PT100 sensors, hollow shafts, and an inductive transducer.

4.1.2 Demagnetization tests

Demagnetization of the magnets in a permanent magnet machine can easily be tested by the locked-rotor method (P7 and P8). It means that the permanent magnets can be demagnetized by the following procedure. First, the machine is heated up at no load, rated speed, and high current condition without cooling. When the rotor temperature has reached near the desired temperature of the magnets, the shaft is locked and predefined current and frequencies are supplied to the machine. The combination of the temperature and the stator field partly demagnetizes the magnets. Finally, the machine is cooled down by rotating at no load and with external cooling. During the heating and cooling processes, the induced voltages are measured. The demagnetization can be defined from these curves. An example, for grade Neorem491a magnets (Neorem, 2010), is shown in Figure 18. Finally, the magnets were also taken out from the machine and the actual demagnetizations were measured for each magnet. More details of this test are explained in P7.

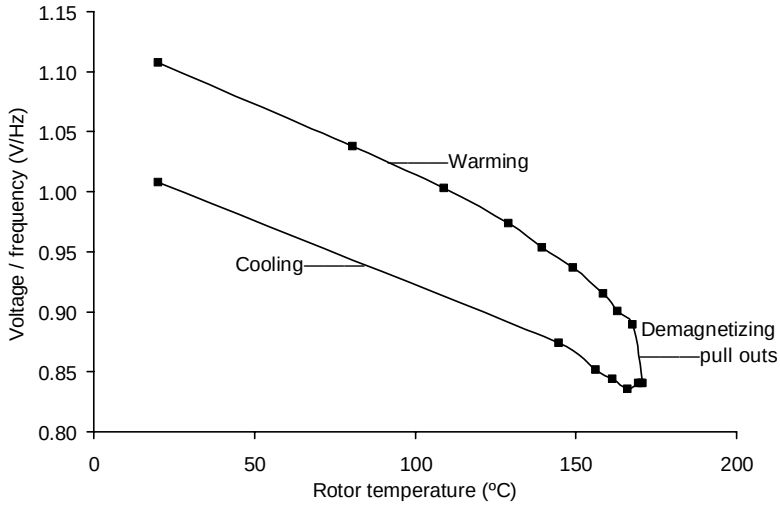

Figure 18: Induced voltage and frequency ratio during a demagnetization process.

4.2 Rotor position definition

Rotor position detection is important for driving synchronous machines. However, the rotor position information is also needed for performing a more accurate analysis of test results, as is done in this dissertation.

A simple way to define the rotor position is to install a rotating shaft sensor. The rotating shaft sensor gives accurate results, but extra equipment is needed. There are also several rotor position definition techniques where direct rotor position measurements are not needed. For example, Matsuo and Lipo (1995) developed rotor position estimating techniques using current measurement. They first defined the inductances of an SRM from the change in the rate of the current during inverted switching. The rotor position is then defined from these inductances.

The air gap flux positions of star-connected induction machines can be defined using the measured first and third harmonics of phase voltages. Kreindler et al. (1994) introduced this method for a direct field orientation controller. For using this method, only six position samples per electrical cycle are needed. Bonanno et al. (1997) extended the use of the stator voltage third harmonic component to a direct self-control scheme for induction motor drives.

However, no studies where the synchronous machine rotor positions were defined by using the third harmonic components of the voltages or the currents and the first harmonics of the current were found during the literature study.

In addition to rotor position estimation techniques being used for controlling frequency converters, they can be used for validating calculation methods, as in this dissertation. In order to gain a deeper understanding of the properties of the machine, some modeling should be done. For good validation, the model needs enough measured parameters: input voltage wave form, current, load angle, and resistance of the stator winding. The load angles are not usually measured directly. However, modern frequency converters define them from the currents by using a machine model. In this chapter an explanation is given of how the right load angle can be approximated from the measured phase currents in a delta connection and from the measured phase voltages in a star connection.

In synchronous machines, the stator flux usually has a clear third harmonic. In a delta connection, it can be seen as a third harmonic of the phase current and, in a star connection, it can be seen as a third harmonic of the phase voltage. The load angle follows the above-mentioned third harmonic and can be defined from the third harmonic. The machines considered here have no stator winding chording (Pyrhönen et al., 2008) which can be used to reduce the third harmonics of phase currents and voltages.

In this chapter, the phenomenon is first demonstrated by modeling the six-pole PMSM with V-shaped permanent magnets. The machine is one comparable to the dovetail design in P5 (frame size 160 mm, supply voltage 360 V, open circuit voltage 262 V, rated power 45 kW, rated speed 6000 1/min). For validating this model, some comparisons between the measured and modeled results are also made for the dovetail PMSM (design in P5) and the dovetail SRM (design in P6).

4.2.1 Method for defining the load angle in delta connection

The phase currents in the delta connection for load angles from 0º to 120º of the V-shaped permanent magnet machine are shown in Figure 19. In all the calculations, the voltage wave form and phase angle are the same. The load angle is defined in such a way that the torque is zero with the load angles of 0º and 180º. The clear third harmonics of currents can be seen for all the loads. The phase angles of the first and the third harmonics are functions of the load angle.

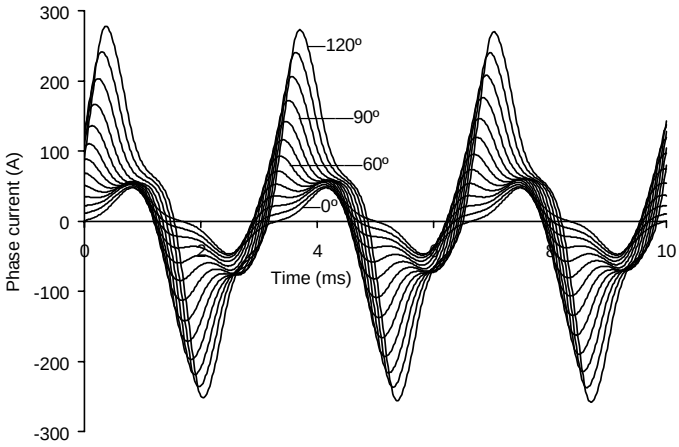

Figure 19: Modeled phase currents at different load angles in the delta-connected V-shaped rotor machine.

If the angles of the first and third harmonic of the current are defined to be zero when the load angle is zero, the load angle can be approximated to be half of the sum of the angles. This is shown in Figure 20.

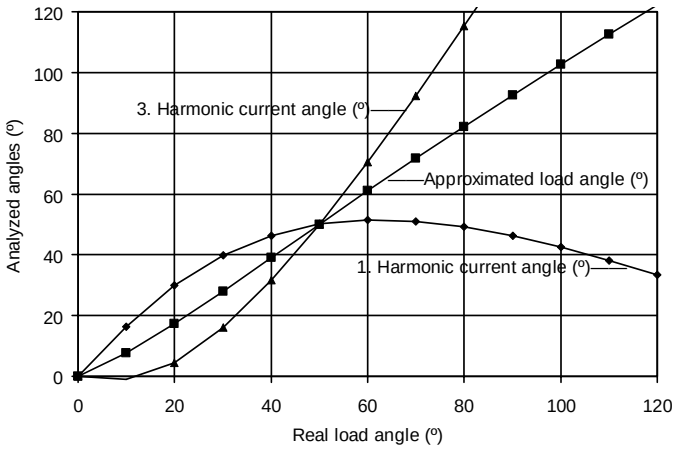

Figure 20: Angles of first and third harmonics of phase currents in the delta-connected V-shaped rotor machine. The approximated load angles are also shown. The real load angles are the load angles of the model.

4.2.2 Method for defining the load angle in star connection

The phase voltages in the star connection for load angles from 0º to 120º of the V-shaped permanent magnet machine are shown in Figure 21. The third harmonics of the voltages increase and move when the load angle increases.

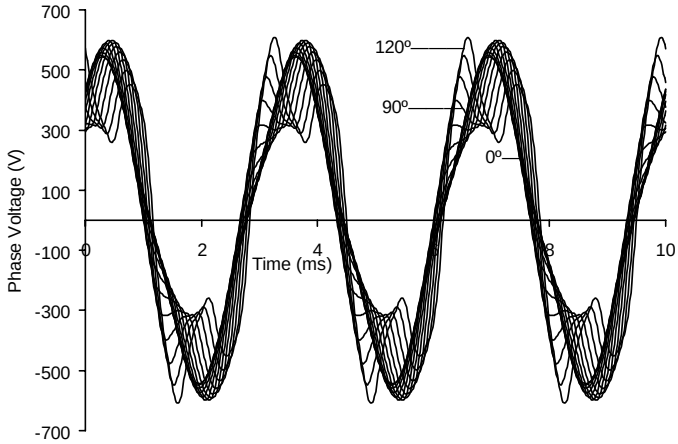

Figure 21: Modeled phase voltages at different load angles in the star-connected V-shaped rotor machine.

If the angles of the first harmonic of the current and the third harmonic of the voltage are defined to be zero when the load angle is zero, the load angle can be approximated to be half of the sum of the angles. This is shown in Figure 22.

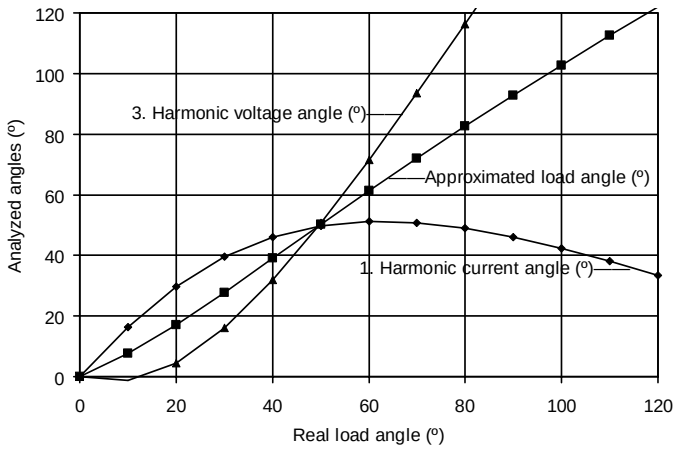

Figure 22: Angles of first harmonic of phase current and third harmonic of phase voltage in the star-connected V-shaped rotor machine. The approximated load angles are also shown. The real load angles are the load angles of the model.

4.2.3 Measured and modeled phase currents of dovetail PMSM

The electrical properties of the dovetail permanent magnet machine (P5) are studied by comparing the measured voltage, the phase current, and the line current to the modeled ones in Figure 23. The wave forms of the measured line and phase currents follow the modeled ones very well. The clear third harmonics of the phase currents can also be seen.

It can be seen that the load angle definition method that is presented is also usable for the dovetail PMSM.

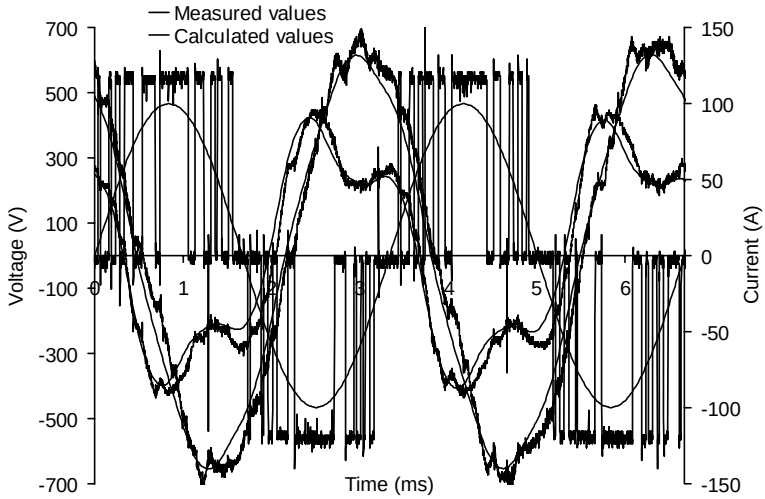

Figure 23: Measured and calculated (smoother curves) voltages, phase currents, and line currents of dovetail PMSM, at speed 6000 1/min.

4.2.4 Measured and modeled phase currents of dovetail SRM

The dovetail SRM (in P6) is modeled with the load angle and voltage which give almost identical phase currents to the measured currents. The measured and calculated currents behave similarly, as can be seen in Figure 24.

The machine is calculated at an electric load angle of 44.0º and the load angle defined from the calculated phase current is 44.4º. The load angle defined from the measured phase current is 44.8º. All the values are near each other. It can be seen that the load angle definition method that is presented is also usable for this dovetail SRM.

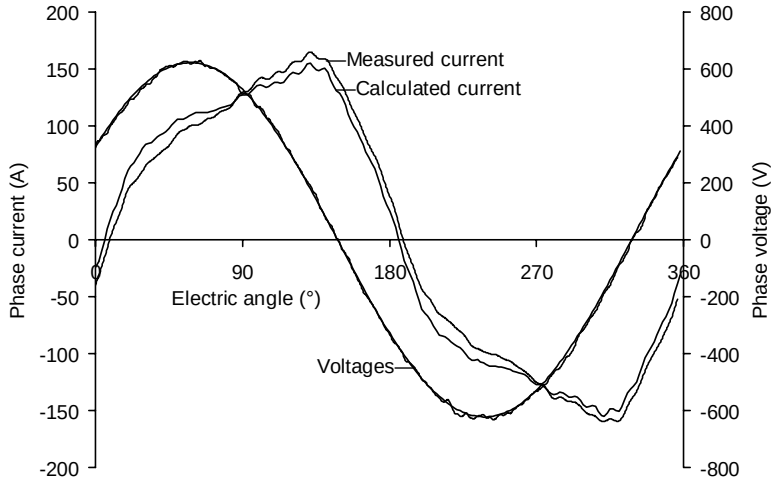

Figure 24: Measured and calculated voltages, phase currents, and line currents of the dovetail SRM.

4.2.5 Conclusion of load angle definitions

In conclusion, the load angles of the designs shown can be defined directly from the measured phase currents and voltages. Other measurements are not needed. This is very useful for the validations of electrical analyzing models.

5 Analysis of tested results

5.1 Overview

For usability validation of the dovetail design of synchronous machines, four dovetail permanent magnet synchronous machines (DPMSM) and two dovetail synchronous reluctance machines (DSRM) are designed and manufactured. These machines are compared with the three conventional permanent magnet synchronous machines with V-shaped magnets (VPMSM) and one bridge fixed synchronous reluctance machine (BSRM). The dovetail and V-shaped rotor structures that are studied are shown in Figure 25. The scale of all the rotors is the same.

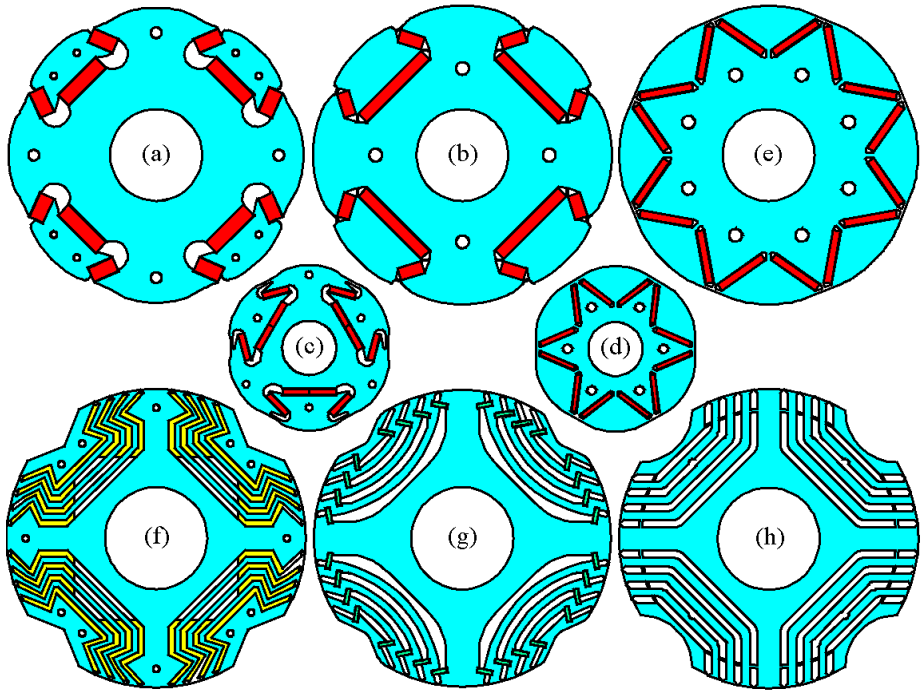

Figure 25: Manufactured PMSM and SRM rotor structures. Five rotors (a, b, c, f and g) are dovetail ones and three rotors (e, d and h) are conventional ones.

The dovetail PMSM prototypes are supported only by the magnets (a) or mainly by the magnets and partly by the bridges between the poles (b, c). The dovetail SRM prototypes are supported by the dovetail shape and glue (f) or non-magnetic steel bars (g). The original V-shaped designs for the two larger dovetail rotors are only slightly different. Therefore only one of them is shown in (e). For the V-shaped designs, compared to the design in (a) and (b), the radial bridges are 6 mm and 5 mm long and the air gap lengths are 3.0 mm and 1.2 mm, respectively. The original design for the smallest dovetail PMSM rotor is shown in (c). The original design for the glued dovetail SRM rotor (f) is shown in (h).

The durability and electrical properties of all the prototypes mentioned above are tested. All the machines have rated input voltages near 360 V, the numbers of stator slots are 72 and 36, and the numbers of poles are 4, 6 and 8. All the PMSMs are water-cooled, with steel or aluminum frames, and all the SRMs are air-cooled, with cast iron frames. The main parameters of the prototype machines are shown in Table 3. However, more details can be found in the publications at the end of the dissertation.

Table 3: Main parameters of the prototype machines.

Machine	Shaft height (mm)	Pole number	Number of bridges	Supporting method	Rated power (kW)	Max. tested speed (1/min)
PM250D4	250	8	4	Magnets, glue, bridges	185	5500
PM250V4	250	8	3	Bridges	185	5500
PM250D0	250	8	0	Magnets, glue	110	4800
PM250V0	250	8	3	Bridges	110	4800
PM160D0	160	6	0	Magnets, glue	45	10000
PM160D2	160	6	2	Magnets, glue, bridges	45	10000
PM160DS	160	6	2	Magnets, sheets, bridges	45	6000
PM160V	160	6	3	Bridges	45	4500
SR280D0	280	4	0	Glue	90	1800
SR280B2	280	4	2	Bridges	90	1500
SR280D2	280	4	2	Bars, bridges	121	4500

To provide an overview of the results of the prototypes, the ratios between the rotor parameters and the results of the dovetail and the original designs are compared in Table 4. The ratios are defined as the dovetail values in relation to the V-shaped values. The compared electrical results are the modeled ones. The thickness and width of the PM rotors mean the total effective thickness and lengths of the magnets seen by the stator. The bridge thickness means the total bridge thickness between the adjacent poles.

The dovetail PMSM rotor without any bridges between the poles (PM250br0) has the same effective thickness and width of the magnets as the original V-shaped rotor. Therefore, the effect of the smaller leakage flux can clearly be seen in the larger open circuit voltage and the lower no-load current. However, the smaller tangential width of every second pole of the dovetail designs reduces the maximum torque. Although the asymmetric poles reduce the maximum torque, the other properties, such as the efficiencies at the rated and partial loads, remain near the same level, as can be seen in Figure 3 and Table III in P5, where the dovetail and dovetail-size V-shaped

designs are compared. The same effects are also present in the other PM results, but there the dovetail designs have wider and thinner magnets, which dominate the difference in the electrical results. In addition, the possibility of designing wider magnets for the dovetail designs gives more design freedom than in the V-shaped designs.

In the dovetail SRM designs (SR280), the thinner and longer flux barriers increase the leakage flux compared to the original design, even though the bridges between the flux barriers are much thinner. Therefore, the electrical properties are lower than in the original SRM. However, the maximum speeds of the dovetail SRMs are clearly greater. The dovetail bar-supported SRM results are not compared in Table 4, because of the complex view of strength, which was discussed in Section 3.5.4.

Table 4: Ratios of modeled properties of dovetail and original designs. (= modeled without bridges)(In …DN: N is the number of bridges in the dovetail design)*

Machine	Magnet thickness	Magnet length	Bridge thickness	Pole width ratio	OC voltage	Maximum torque	No load current	Speed increase
PM250D4	0.80	1.30	0.51	0.84	1.16	0.82	1.34	1.01*
PM250D0	1.00	1.00	0.00	0.84	1.11	0.90	0.31	1.00
PM160D2	0.78	1.28	0.37	0.65	1.29	0.82	0.35	0.92
PM160D0	0.78	1.28	0.00	0.65	1.36	0.85	0.24	0.91
SR280D0	-	-	0.00	1.00	-	0.82	1.34	1.54

Next, all the prototypes are introduced, with some comments on the usefulness of their structure. More detailed descriptions are given in the publications.

5.2 Eight-pole PM machine with radial and tangential bridges between poles

The first dovetail rotor to be manufactured is shown in Figure 26 (left). In Figure 26 (right), the end plates are removed after the tests. The details of the comparisons of the prototypes are shown in P2. In this dovetail design, the bridges between the poles are kept in every corner of the magnets, so the number of bridges between the poles is larger than in the V-shaped design that it is compared to. However, the total flux leakage route is much thinner in the dovetail design, as can be seen in Table 4 (PM250D4). The poles are mainly supported by the magnets and partly by the bridges. This dovetail rotor is manufactured with the same method as the original V-shaped design. However, in this dissertation, it has been shown that at least the inner bridges are not needed for increasing the strength. The inner bridges also worsen the electric properties of the rotor.

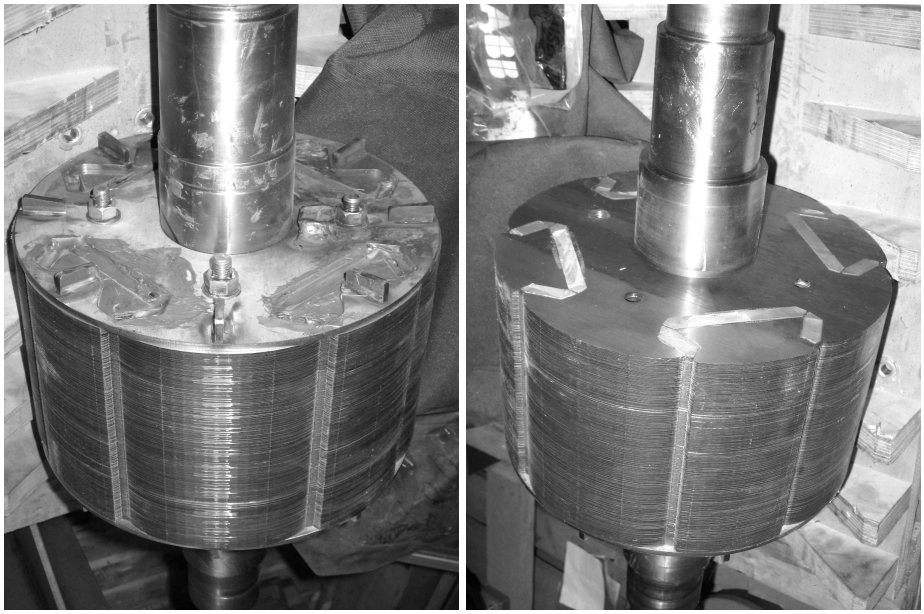

Figure 26: Dovetail rotor with four supporting bridges after test and with and without the end plate.

5.3 Eight-pole PM machine without any bridges between poles

Because some of the bridges might be unnecessary, a dovetail PM machine where the poles are supported only by the magnets is designed and manufactured (PM250D0) (Figure 27). It is shown to be a good choice for the dovetail design in P3. However, manufacturing it is quite difficult, because of the strong magnetic forces during the manufacturing process, especially when it was desired to install the poles with the magnets into the rotor.

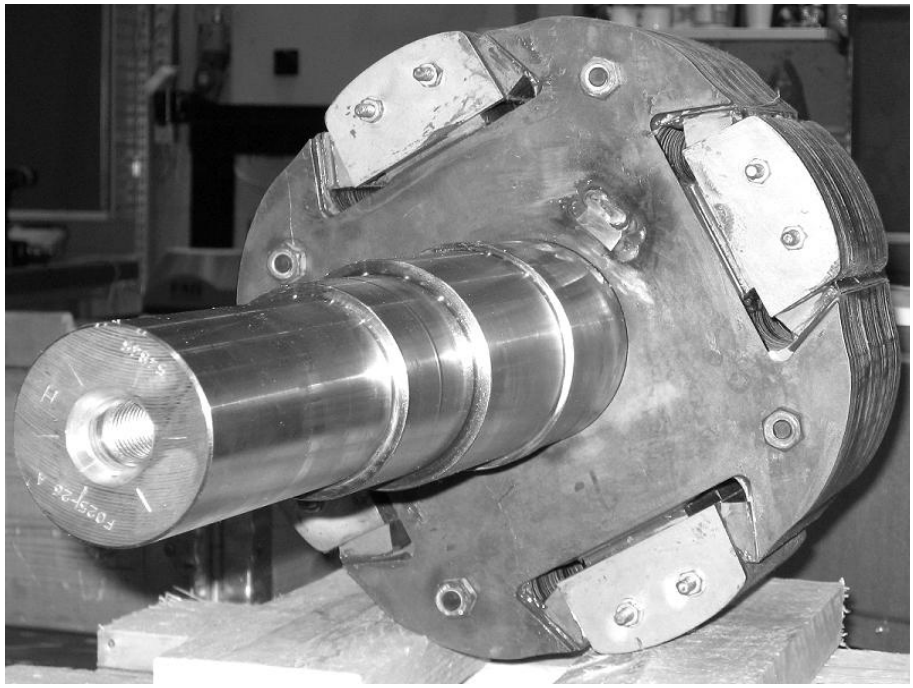

Figure 27: Dovetail rotor without supporting bridges.

5.4 Six-pole PM machine

In order to avoid the manufacturing difficulties of the dovetail PM machine, it is useful to leave thin tangential bridges between the poles to the dovetail rotor. Therefore, a six-pole dovetail machine is designed and manufactured. Studies of this design are presented in P4, P5, P7, and P8.

In P4 and P5, the magnets are assembled by using glue on the largest surfaces of the magnets (PM160D2) (Figure 28 (left)). In P7 and P8, the magnets are assembled by using non-magnetic electrical sheets between the magnets and the electrical sheets and the magnets are locked by glue only at the ends (PM160DS) (Figure 28 (middle)). This installation makes it possible to change the magnets between the tests, as was done in the studies in P7 and P8. Both the installation methods are proven to be strong enough for the speeds considered. All the magnets survived all the tests mentioned in P4, P5, P7, and P8.

This structure is proven to be superior over the conventional design with the V-shaped magnets, as is shown in P5.

The tests are continued for a glued rotor where the tangential bridges are cut away (PM160D0) (Figure 28 (right)). The superiority of this design can be seen from Table 4.

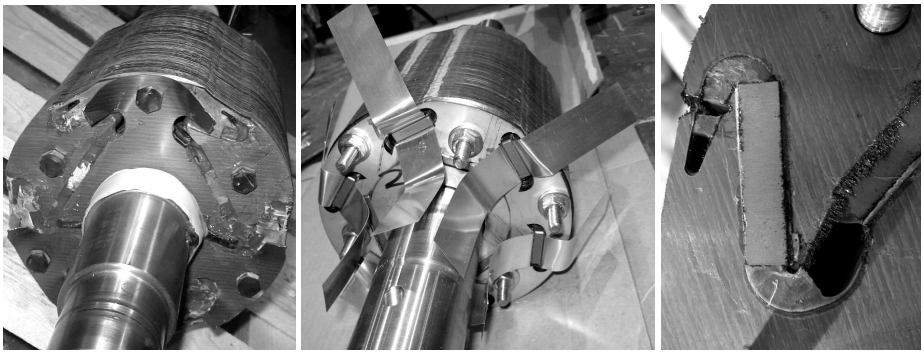

Figure 28: Dovetail rotor with two supporting bridges and with two installation methods used for the magnets and with cut tangential bridges.

5.5 Synchronous reluctance machines without bridges between flux barriers

A dovetail SRM with magnetically separated flux paths is introduced in P6. The structure is supported by the dovetail form-blocked method, where epoxy filler separates the supporting parts (SR280D0). The main supporting stress of the glue is the compressive stress. The rotor before gluing and machining is shown in Figure 29 (right). The rotor after gluing and machining is shown in Figure 29 (left). Note that the bridges between the flux paths which helped in the assembly of the rotor before gluing are finally machined away.

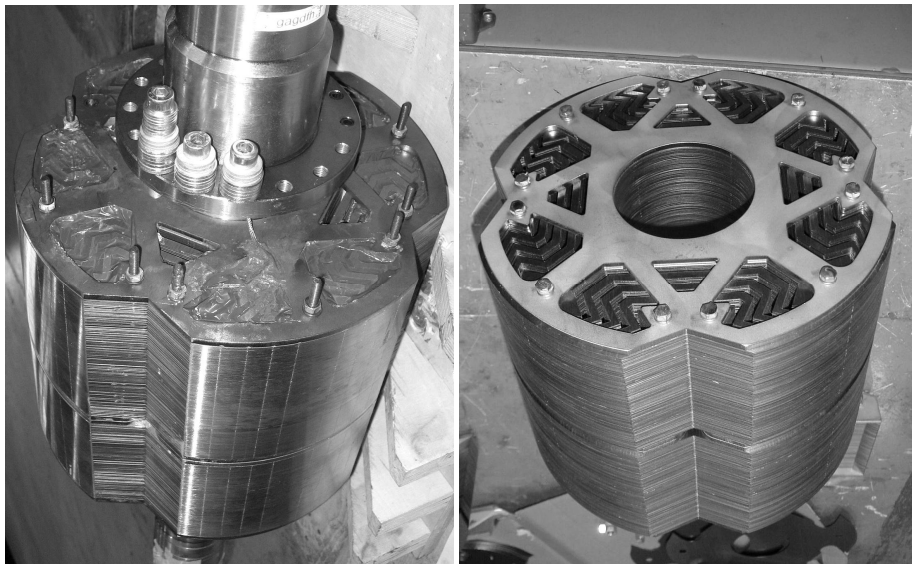

Figure 29: Dovetail SRM rotor supported by glue in the flux barriers.

However, in the tests, it was seen that when glue is used as a filler material the heating of the rotor might cause problems. So, during the heat-up test at 105 kW and 1500 1/min, the epoxy filler was partly melted around the warmest points of the rotor and it was thrown out from the rotor. Melting of the epoxy filler appeared near the bolts because the induced currents warmed them up.

It was suggested that the problem could be solved by using the other heat-resistant filler materials in P6 or non-magnetic metal bars, as shown in the next chapter. This machine might work if the bolts are taken away after the gluing of the rotor, but this was not tested.

5.6 Synchronous reluctance machines with supporting bars

The dovetail SRM where the flux paths are supported by non-magnetic steel bars (SR280D2) is introduced in this dissertation. Figure 30 (right) presents the internal rotor structure during the installation and Figure 30 (left) presents the final rotor. The machine is designed for an output power of 160 kW and a speed of 4500 rpm. However, the highest measured output power is 121 kW and the speed 4500 rpm, because during the load tests, when the rotor was warming up, the rotor touched the stator.

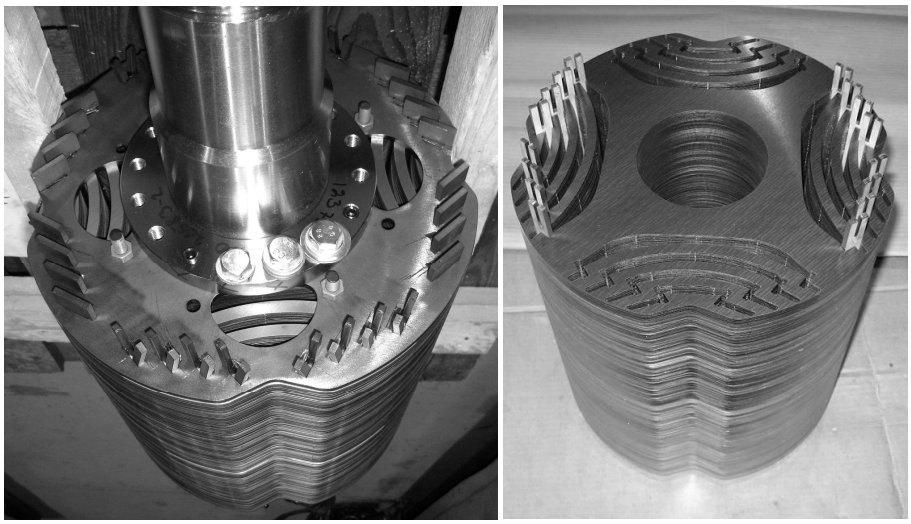

Figure 30: Dovetail SRM rotor supported by non-magnetic steel bars in the flux barriers during installation and after balancing.

Problems first appeared during the balancing process, when all the supported flux paths and the supporting bars moved outwards and came into tight contact with each other. All tolerances disappeared. Therefore, the maximum diameter of the rotor was increased from 290.9 mm to 293.7 mm. The maximum measured increase of the radius is then 1.4 mm, while the calculated expected value is $4 \times 0.2\text{mm}/\cos(55°) = 1.4$ mm. Thus the deformations were exactly what were expected. Therefore, the expected smallest air gap was reduced from 2.0 mm to 0.6 mm.

During the load tests, when the motor was warmed up, the rotor touched the stator and the machine was broken. The rotor was damaged only from the non-drive end side. Because the non-magnetic plate partly supports the middle of the rotor, the two axial sides of the rotor behave mechanically separately. One end does not affect the other. However, the diameter and form of the other end of the rotor remained the same. Therefore, the conclusion can be drawn that the damage is only caused by too small an air gap.

5.7 Conclusion of the prototype studies

The dovetail synchronous machines were successfully tested. Although some of them finally broke down, enough knowledge was collected for validation of the mechanical and electromagnetic analysis models. The usability and limits of the permanent magnets, steel bars and sheets, and glue with different combinations for supporting parts of the PMSM and SRM rotors were sought.

The best PMSM rotor solution (which the author recommends using) is glued permanent magnets with two thin tangential bridges. The glue smooths the peaks of stress resulting from the deviations between the surfaces; the magnets are then protected. Some bridges help the manufacturing process. The tangential bridges are better than radial ones, because they allow more space for the supported parts to move outwards without increasing the stresses so much as in the radial bridges. With the use of tangential bridges, the stress distribution is also smoother.

6 Discussion

This chapter is the summary and discussion of the results of this dissertation. First, a short summary of the work is given. Then conclusions are drawn about the significance of the results and research. Finally, open issues and the future of the dovetail designs are discussed.

6.1 Summary of the work

Several dovetail SRM and PMSM prototypes were designed during this work. Five different dovetail machines were designed and six dovetail prototypes were manufactured. These machines were compared with four commonly used designs where the parts of the rotors are fixed by bridges. Comparisons were made by several tests and by electromagnetic and mechanical FEA. Some analytical methods were developed.

6.2 Significance of the research

The main significance of this research is to show that the commonly used bridge-fixed SRM and PMSM rotors could be changed to dovetail (form-blocked) structures, which have a better combination of electrical and mechanical properties. Both the electrical and mechanical properties could be improved simultaneously. The dovetail PMSM structures can also be used to reduce the amount of magnetic material because of the smaller leakage flux compared to the conventional bridge-fixed designs.

The calculation principles for validating the improved properties are also developed. In particular, the methods used for defining the mechanical strength of the dovetail rotor are considered in depth, because the strength analysis principles are more complicated in the dovetail designs than in the bridge-fixed ones.

The relations between the mechanical and the electrical properties have also been studied. It has been shown that the dovetail PMSM machine has the best mechanical and electrical properties with similar structures, while in the original V-shaped structures, increasing the mechanical strength causes the electrical properties to deteriorate.

In this work, two analytical methods that are used rarely or not at all are successfully utilized.

The asymmetric torque distribution of the dovetail consequent pole rotor was studied by the normalized local tangential force density. This method makes it possible to analyze the torque distribution in the air gap without the direct effect of the stator slots. Therefore, the goodness of the rotor structure can be seen easily.

The load angles of PMSMs and SRMs can be defined from the measured first and third current harmonics, when the machine is delta-connected. This method is validated by modeling and used for finding the right analytical parameters more effectively. The known load angles of tested results greatly increase the possibilities for validating the analytical methods. There is one parameter more, which is easy to analyze from the measurements, to include in the analytical models.

The mechanical durability of Nd-Fe-B magnets in dovetail PMSM rotors was proven by testing. No indications of mechanical changes in the magnets were seen during any of the tests. The magnets were also shown not to be critical for the strength of dovetail PMSM rotors.

In conclusion, the principles for the design and analysis of dovetail PMSMs and SRMs are developed. The knowledge of how the dovetail PMSM and SRM rotor strength should be analyzed was stablished.

6.3 Open issues and future work

The electrical properties of the dovetail PMSM and SRM can be analyzed by the methods used and developed in this work. They are ready to be used in the design procedure.

The mechanical durability is also proven by modeling and testing. However, it was proved by modeling with a high safety margin and the tests only lasted for a few days. The real strength limits can only be found by long-term tests. Then the safe maximum speeds may also be increased. One open question for rotor speed durability is how the glue between the magnets and rotor iron behaves. For example, does the glue wear away during long-term usage? Tests of long duration might also reveal unknown problems.

Although dovetail SRMs are discussed in this dissertation, the main focus was on PMSMs. Therefore some issues for strength definition are left open, as could be seen in Section 3.5.4. Comparisons with bridge-fixed designs where the bridges are in the same positions as in Figure 2(c) should be made in order to obtain a better view.

The open issue when designing electric motors is always to have slightly better designs. Figure 31 shows a dovetail SRM and a dovetail PMSM design for possible dovetail rotor structures in future. The dovetail SRM is modeled to be stronger and have better electrical properties than the design presented in Section 5.6. The dovetail PMSM shows one design alternative for the positions of the magnets. In addition, by using optimizing algorithms stronger and more efficient structures could be found.

The most interesting future issue is to install the first dovetail PMSM and dovetail SRM to real applications. The solutions and analytical methods developed in this dissertation, which are especially suitable for dovetail solutions, are very promising for propelling electrical machine development forward.

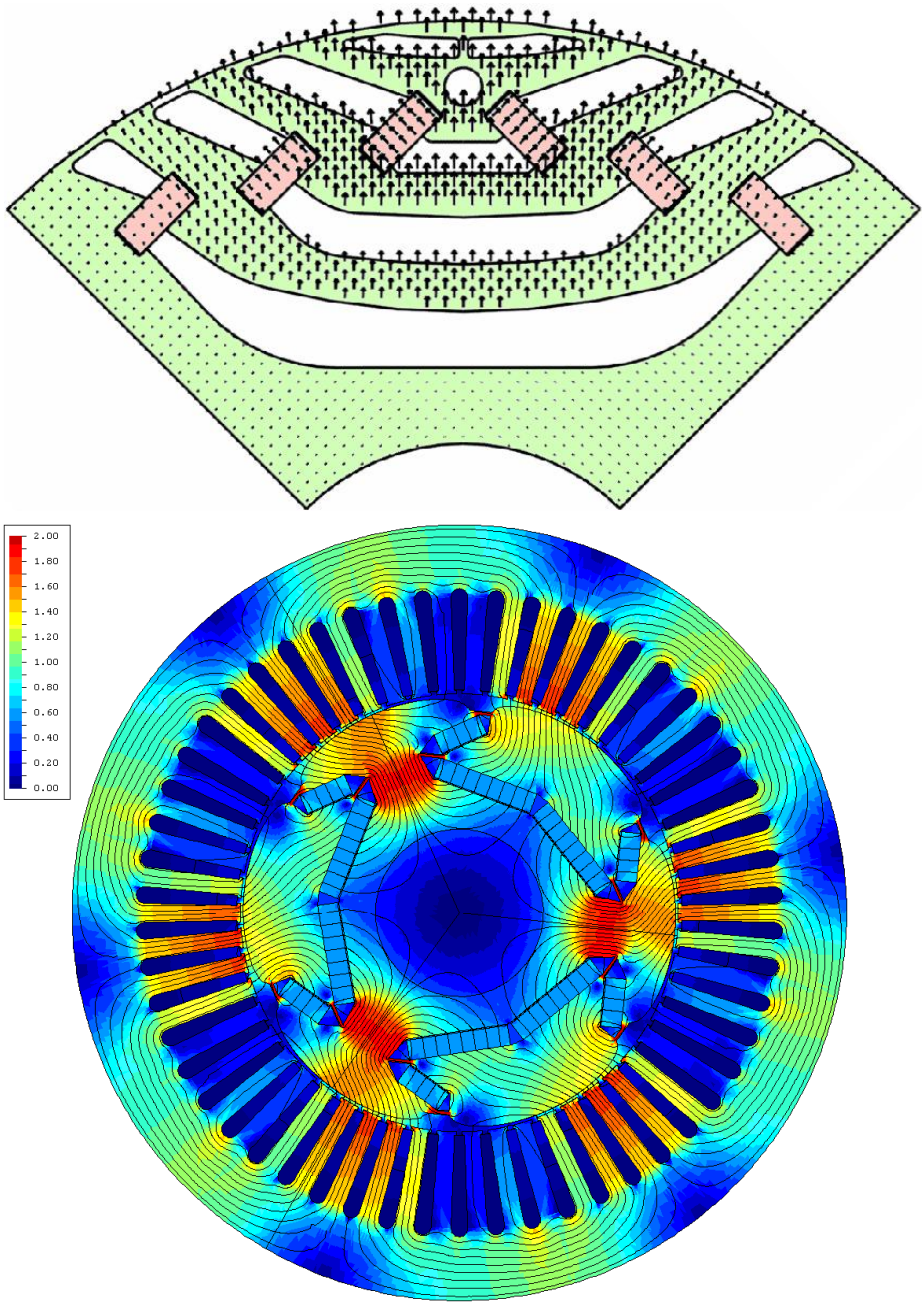

Figure 31: Possible future solutions for dovetail SRM (modeled ¼-rotor with displacement arrows) and PMSM machines (with analyzed flux densities and lines).

References

ACS. 2010. Frequency converters. Available at www.abb.com.

Amemiya J., Chiba A., Dorrell D.G., Fucao T. 2005. Basic characteristics of a consequent-pole-type bearingless motor. IEEE Transactions on Magnetics, Vol. 41, No. 1, January 2005, pp. 82-89.

Arkkio A. 1987. Analysis of induction motors based on the numerical solution of the magnetic field and circuit equations. Ph.D. thesis. Helsinki University of Technology. Finland. 97 p. Available in http://lib.tkk.fi/Diss/198X/isbn951226076X/

Arkkio, A., Niemenmaa, A. 1992. Estimation of losses in cage induction motors using finite element techniques," in Proceedings of the International Conference on Electrical Machines - ICEM'92, Manchester, U.K., Vol. 2, 1992, pp. 317-321.

Barcaro M., Bianchi N., Magnussen F. 2010. Design considerations to maximize performance of and IPM motor for a wide flux-weakening region. International Conference on Electrical Machines – ICEM'10, September 2010.

Belahcen A. 2004. Magnetoelasticity, magnetic forces and magnetostriction in electrical machines. Ph.D. thesis. Helsinki University of Technology. Finland, 115p. Available in http://lib.tkk.fi/Diss/2004/isbn9512271850/.

Belmans R., Verdyck D., Geysen W. 1989. Optimization of permanent magnet machines with respect to torque and audible noise. International Conference on Electrical Machines and Drives, September 1989, pp. 80-84.

Bianchi N., Bolognani S. 2002. Interior PM synchronous motor for high performance applications. Proceedings of Power Conversion Conference, Vol. 1, April 2002, pp. 148-153.

Binns K.J., Chaaban F.B., Hameed A.A.K. 1993. Major design parameters of a solid canned permanent magnet motor with skewed magnets. IEE Proceedings-B, Vol. 140, No. 3, May 1993, pp. 161-165.

Boldea I., Tutelea L., Pitic C.I. 2004. PM-assisted reluctance synchronous Motor/Generator (PM-RSM) for mild hybrid vehicles: electromagnetic design. IEEE Transactions on Industry Applications, Vol. 40, No. 2, March/April 2004, pp. 492-498.

Boldea I., Pitic C.I., Lascu C., Andreescu G.-D., Tutelea L., Blaabjerg F., Sandholdt P. 2006. DTFC-SVM motion-sensorless control of a PM-assisted reluctance synchronous machine as starter-alternator for hybrid electric vehicles. IEEE Transactions on Power Electronics, Vol. 21, No. 3, May 2006, pp. 711-719.

Bolognesi P., Papini F., Biagini V. 2010. Consequent-pole brushless machines featuring uneven magnet-pole width ratio. International Conference on Electrical Machines – ICEM'10, September 2010.

Bomela X.B., Kamper M.J. 1999. Effect of stator chording and rotor skewing on average torque and torque ripple of reluctance synchronous machine. Africon, 1999 IEEE, Vol. 2, 1999, pp. 687-690.

Bomela X.B., Kamper M.J. 2002. Effect of stator chording and rotor skewing on performance of reluctance synchronous machine. IEEE Transactions on Industry Applications, Vol. 38, No. 1, January/February 2002, pp. 91-100.

Bonanno F., Consoli A., Raciti A., Testa A. 1997. An innovate direct self-control scheme for induction motor drives. IEEE Transactions on Power Electronics, Vol. 12, No. 5, September 1997, pp. 800-806.

Cao W., Huang X., French I. 2009a. Design of a 300-kW calorimeter for motor loss measurement. IEEE Transactions on Instrumentation and Measurement, Vol. 58, No. 7, July 2009, pp. 2365-2367.

Cao W., Bradley K.J., Ferrah A. 2009b. Development of a high-precision calorimeter for measuring power loss in electrical machines. IEEE Transactions on Instrumentation and Measurement, Vol. 58, No. 3, March 2009, pp. 570-577.

Castagnini A., Garavaglia M., Moriconi F., Secondo G. 2002. Development of a very high speed and power synchronous PM motor. International Conference on Electrical Machines – ICEM'02, September 2002.

Castagnini A., Leone I. 2002. Test results of a very high speed PM brushless motor. International Conference on Electrical Machines – ICEM'02, September 2002.

Chalmers B.J., Musaba L. 1998. Design and field-weakening performance of a synchronous reluctance motor with axially laminated rotor. IEEE Transactions on Industry Applications, Vol. 34, No. 5, September/October 1998, pp. 1034-1041.

COMSOL Multiphysics software. 2010. Available at www.comsol.com

Coulomb J.L. 1983. A methodology for the determination of global electromechanical quantities from a finite element analysis and its applications to the evaluation of magnetic forces torques and stiffness. IEEE Transactions on Magnetics, Vol. 19, No. 6, November 1983, pp. 2514-2519.

Cruickshank A.J.O., Menzies R.W., Anderson A.F. 1966. Axially laminated anisotropic rotors for reluctance motors. IEE Proceedings, Vol. 113, No. 12, December 1966, pp. 2058-2060.

Dutta R., Rahman M.F. 2008. Design and analysis of an interior permanent magnet machine with very wide constant power operation range. IEEE Transactions on Energy Conversion, Vol. 23, No. 1, March 2008, pp. 25-33.

El-Refaie A.M., Manzke R., Jahns T.M. 2004. Application of bi-state magnetic material to automotive offset-coupled IPM starter/alternator machine. IEEE Transactions on Industry Applications, Vol. 40, No. 3, May/June 2004, pp. 717-725.

El-Refaie A.M. 2005. High speed operation of permanent magnet machines. Doctoral thesis, University of Wisconsin-Madison, USA.

El-Refaie A.M., Jahns T.M. 2005. Application of bi-state magnetic material to an automotive IPM starter/alternator machine. IEEE Transactions on Energy Conversion, Vol. 20, No. 1, Mar 2005, pp. 71-79.

Evans S.A. 2008. Novel rotor design for interior permanent magnet brushless machines: initial investigation. International Conference on Electrical Machines – ICEM'08, September 2008.

Evans S.A. 2010. Salient pole shoe shapes of interior permanent magnet synchronous machines. International Conference on Electrical Machines – ICEM'10, September 2010.

FLUX software. 2010. Available at www.cedrat-groupe.com

Fukami T., Momiyama M., Shima K., Hanaoka R., Takata S. 2008. Steady-state analysis of a dual-winding reluctance generator with a multiple-barrier rotor. IEEE Transactions on Energy Conversion, Vol. 23, No. 2, June 2008, pp. 492-498.

Fukao T., Chiba A., Matsui M. 1989. Test results on a super-high-speed amorphous-iron reluctance motor. IEEE Transactions on Industry Applications, Vol. 25, No. 1, January/February 1989, pp. 119-125.

Gan J., Chau K.T., Chan C.C., Jiang J.Z. 2000a. A new surface-inset permanents-magnet brushless dc motor drive for electric vehicles. IEEE Transactions on Magnetics, Vol. 36, No. 5, September 2000, pp. 3810-3818.

Gan J., Chau K.T., Chan C.C., Jiang J.Z. 2000b. Design and analysis of a new permanent magnet brushless DC machine. IEEE Transactions on Magnetics, Vol. 36, No. 5, September 2000, pp. 3353-3356.

Haataja J., Pyrhönen J., Niemelä M., Neuvonen M. 2002. Measurement of synchronous reluctance and induction motors in variable speed drives utilizing IEEE 112 B test method. International Conference on Electrical Machines – ICEM'02, September 2002.

Halberg J. 2005. Conceptual evaluation and design of a direct-driven mixer. Master thesis. Department of Mechanical Engineering, Linköpings University, Linköping, Sweden.

Heikkilä T. 2002. Permanent magnet synchronous motor for industrial inverter applications - analysis and design. Doctoral thesis. Lappeenranta University of Technology. 109 p.

Henneberg G., Domack S., Berndt J. 1993. Influence of end winding leakage in permanent magnet excited synchronous machines with asymmetrical rotor design. Sixth International Conference on Electrical Machines and Drives (Conf. Publ. No. 376), September 1993, pp. 305-311.

Hershberger D. 1982. Electronically commutated motor, stationary and rotatable assemblies therefore, and lamination. US4327302 (A), April 1982.

Hofmann H., Sanders S.R. 1996. Synchronous reluctance motor/alternator for flywheel energy storage systems" in Proc. IEEE Power Electronics in Transportation Workshop, 1996, pp. 199-206.

Hofmann H., Sanders S.R. 2000. High-speed synchronous reluctance machine with minimized rotor losses. IEEE Transactions on Industry Applications, Vol. 36, No. 2, March/April 2000, pp. 531-539.

Horton J.A., Herchenroeder J.W., Wright J.L., Easton D.S. 1996. Fracture toughness of Nb12Fe14B magnets. Material Transactions on JIM, Vol. 37, April 1996, pp. 860-863.

Hwang C.-C., Cho Y.H. 2001. Effects of leakage flux on magnetic fields of interior permanent magnet synchronous motors. IEEE Transactions on Magnetics, Vol. 37, No. 4, July 2001, pp. 3021-3024.

Jahns T.M., Kliman G.B., Neumann T.W. 1986. Interior permanent-magnet synchronous motors for adjustable-speed drives. IEEE Transactions on Industry Applications, Vol. IA-22, No. 4, July/August 1986, pp. 738-747.

Jahns T.M., Van Nocker R.C. 1989. Electric controls for a high-performance EHA using an interior permanent magnet motor drive. Proceedings of the IEEE 1989 National Aerospace and Electronics Conference - NAECON 1989, Vol. 1, 1989, pp. 346-354.

Jacques S.M., Pascal G. 2001. Rotor for electrical machine, comprises rotor laminations shaped to define hour glass shaped cavities in the rotor face which house laminated pole pieces and pairs of permanent magnets," Patent application FR2802726 (A1), June 22, 2001.

Jayawant B.V., Maynard M., Anbarasu R. 1995. Design of high speed permanent magnet machines in magnetic bearings. IEE Conference Publications, Vol. 412, September 1995, pp. 418-422.

Junak J., Ombach G. 2010. Performance optimization of the brushless motor with IPM rotor for automotive applications. International Conference on Electrical Machines – ICEM'10, September 2010.

Kamiya M. 2005. Development of traction drive motors for the Toyota hybrid system. Available at http://www.e-mobile.ch/pdf/2005/321.pdf

Knauf A., Vollmerr R. 2003. Rotor for a permanent magnet synchronous machine. US2003173853 (A1), September 2003.

Kolehmainen J. 2005. Finite element analysis of two PM-Motors with buried magnets. International Symposium on Electric Fields in Mechatronics, Electrical and Electronic engineering – ISEF'05, September 2005.

Kolehmainen J. 2008a. Rotor for a permanent-magnet electrical machine. WO Patent 2008025873 (A1), March 6, 2008, and FI Patent 119457 (B1), November 14, 2008.

Kolehmainen J. 2008b. Rotor for electric machine," WO Patent 2008037849 (A1), April 3, 2008, and FI Patent 118940 (B1), May 15, 2008.

Kostko J.K. 1923. Polyphase reaction synchronous motors. Journal of American Institute of Electrical Engineers, Vol. 42, November 1923, pp. 1162-1168.

Kreindler L., Moreira J.C., Testa A., Lipo T.A. 1994. Direct field orientation controller using stator phase voltage third harmonic. IEEE Transactions on Industry Applications, Vol. 30, No. 2, March/April 1994, pp. 441-447.

Lamghari-Jamal M.-I., Fouladgar J., Zaim E.-H., Trichet D. 2006. A magneto-thermal study of a high speed synchronous reluctance machine. IEEE Transactions on Magnetics, Vol. 42, No. 4, April 2006, pp. 1271-1274.

Lee J.H., Kim J.G., Hyun D.S. 1999. Effect analysis of magnet on Ld and Lq inductance of permanent magnet assisted synchronous reluctance motor using finite element method. IEEE Transactions on Magnetics, Vol. 35, No. 3, May 1999, pp. 1199-1202.

Lee J.H., Kim D.H., Park I.H. 2003. Minimization of higher back-EMF harmonics in permanent magnet rotor using shape design sensitivity with B-spline parameterization. IEEE Transactions on Magnetics, Vol. 39, No. 3, May 2003, pp. 1269-1272.

Li W., Li A.H., Wang H.J. 2005. Anisotropic fracture behavior of sintered rare-earth permanent magnets. IEEE Transactions on Magnetics, Vol. 41, No. 8, August 2005, pp. 2339-2342.

Li W., Li A.H., Wang H.J., Pan W., Chang H.W. 2009. Study on strengthening and toughening of sintered rare-earth permanent magnets. Journal of Applied Physics, Vol. 105, 07A703, 2009

Lipo T.A., Krause P.C. 1967. Stability analysis of a reluctance synchronous machine. IEEE Transactions on Power Apparatus and Systems, Vol. 86, No. 7, July 1967, pp. 825-834.

Lipo T.A. 1991. Synchronous reluctance machine a viable alternative for AC drives. Electric Machines and Power Systems, Vol. 19, 1991, pp. 659-671.

Lovelace E.C., Jahns T.M., Lang J.H. 2000. Impact of saturation and inverter cost on interior PM synchronous machine drive optimization. IEEE Transactions on Industry Applications, Vol. 36, No. 3, May/June 2000, pp. 723-729.

Lovelace E.C., Jahns T.M., Keim T.A., Lang J.H. 2004. Mechanical design considerations for conventionally laminated high speed interior PM synchronous machine rotors. IEEE Transactions on Industry Applications, Vol. 40, No. 3, May/June 2004, pp. 806-812.

Marino M. 2009. Analytical modeling and optimization of a radial permanent magnets synchronous machine. International Conference on Energy Efficiency in Motor Driven Systems, September, 2009.
Available at http://www1.cetim.fr/eemods09/pages/programme/049-Marino-final.pdf

Matsuo T., Lipo T.A. 1994. Rotor design optimization of synchronous reluctance machine. IEEE Transactions on Energy Conversion, Vol. 9, No. 2, June 1994, pp. 359-365.

Matsuo T., Lipo T.A. 1995. Rotor position detection scheme for synchronous reluctance motor based on current measurements. IEEE Transactions on Industry Applications, Vol. 31, No. 4, July/August 1995, pp. 860-868.

Meier F. 2008. Permanent-magnets synchronous machines with non-overlapping concentrated windings for low-speed direct-drive applications. Ph.D. thesis. Royal Institute on Technology. Sweden. Available at

http://www.ee.kth.se/php/modules/publications/reports/2008/TRITA-EE_2008_041.pdf

Morimoto S., Sanada M., Takeda Y. 1996. Inverter-driven synchronous motors for constant power. IEE Industry Applications Magazine, November/December 1996, pp. 18-24.

Morimoto S., Sanada M., Takeda Y. 2001. Performance of PM-assisted synchronous reluctance motor for high-efficiency and wide constant-power operation. IEEE Transactions on Industry Applications, Vol. 37, No. 5, September/October 2001, pp. 1234-1240.

Moses A.J. 1990. Electrical steels: past, present and future developments. IEE Proceedings-A, Vol. 137, No. 5, 1990, pp. 233-245.

Nedjar B., Hlioui S., Vido L., Gabsi M., Amara Y., Miraoui A. 2010. Magnetic circuit applied to a unipolar PMSM. International Conference on Electrical Machines – ICEM'10, September 2010.

Neorem. 2010. Neorem Magnets. Available at www.neorem.fi.

Niazi P. 2005. Permanent assisted synchronous reluctance motor design and performance improvement. Ph.D. thesis. Texas A&M University. USA. 136 p.

Ouyang W., Zarko D., Lipo T.A. 2006. Permanent magnet machine design practice and optimization Industry Applications Conference, 2006. 41st IAS Annual Meeting. Conference Record of the 2006 IEEE, Vol. 4, pp. 1905 – 1911.

Parsa L., Hao L. 2008. Interior permanent magnet motors with reduced torque pulsation. IEEE Transactions on Industrial Electronics, Vol. 55, No. 2, February 2008, pp. 602-609.

Platt D. 1992. Reluctance motor with strong rotor anisotropy. IEEE Transactions on Industry Applications, Vol. 28, No. 3, May 1992, pp. 652-658.

Pyrhönen J., Jokinen T., Hrabovcová V. 2008. Design of rotating electrical machines. Wiley, United Kingdom, 2008, pp. 72-80.

Ruoho S., Arkkio A. 2007. Mixed-Grade Pole Design for permanent magnet synchronous machines. ACEMP'07 and ELECTROMOTION'07, September 2007.

Ruoho S., Dlala E., Arkkio A. 2007. Comparison of Demagnetization Models for Finite-Element Analysis of Permanent-Magnet Synchronous Machines. IEEE Transactions on Magnetics, Vol. 43, No. 11, November 2007, pp. 3964-3968.

Ruoho S., Arkkio A. 2008. Partial demagnetization of permanent magnets in electrical machines caused by an inclined field. IEEE Transactions on Magnetics, Vol. 44, No. 7, July 2008, pp. 1773-1778.

Ruoho S., Kolehmainen J., Ikäheimo J. 2008. Anisotropy of resistivity of Nd-Fe-B magnets - consequences in eddy-current calculations. Workshop on Rare Earth Permanent Magnets and Applications - REPM'08, September 2008.

Ruoho S., Santa-Nokki T., Kolehmainen J., Arkkio A. 2009. Modeling magnet length within 2D finite-element analysis of electric machines. IEEE Transactions on Magnetics, Vol. 45, No. 8, August 2009, pp. 3114-3120.

Saitz J. 2001. Magnetic field analysis of electrical machines taking ferromagnetic hysteresis into account. Ph.D. thesis. Helsinki University of Technology. Finland, 123 p. Available in http://lib.tkk.fi/Diss/2001/isbn9512256908/.

Salo J., Heikkilä T., Pyrhönen J., Haring T. 2000. New Low-Speed High-Torque Permanent Magnet Synchronous Machine with Buried Magnets. International Conference on Electrical Machines – ICEM'00, September 2000.

Sibande S.E., Kamber M.J., Wang R., Rakgati E.T. 2004. Optimal design of a PM-assisted rotor for a large power reluctance synchronous machine. IEEE AFRICON Conference Proceedings, Vol. 2, Botswana, September 2004, pp. 793-797.

Sibande S.E., Kamber M.J., Wang R. 2006. Design and performance evaluation of a medium power PM-assisted reluctance synchronous traction machine using bonded PM-sheets. SAIEE Africa Research Journal, Vol. 97, No. 1, March 2006, pp. 14-21.

Soong W.L, Staton D.A., Miller T.J.E. 1995. Design of a new axially-laminated interior permanent magnet motor. IEEE Transactions on Industry Applications, Vol. 31, No. 2, March/April 1995, pp. 358-367.

Soong W.L., Ertugrul N. 2002. Field-weakening performance of interior permanent-magnet motors. IEEE Transactions on Industry Applications, Vol. 38, No. 5, September/October 2002, pp. 1251-1258.

Spooner E., Williamson A. 1996. Modular, permanent-magnet wind-turbine generators. Conference Record of the 1996 IEEE Industry Applications Conference, IAS '96., Vol. 1, 1996, pp. 497-502.

Stumberger B., Hamler A., Trlep M., Jesenik M. 2001. Analysis of interior permanent magnet synchronous motor designed for flux weakening operation. IEEE Transactions on Magnetics, Vol. 37, No. 5, September 2001, pp. 3644-3647.

Suh H.S., Lee W.W., Jung Y.G, Han H.S., Park K.H., Chung C.W., Chun C.H., Han K.S. 2006. Physical design of the 2MW generator for KBP-2000M. European Wind Energy Conference & Exhibition – EWEC'06, February/March 2006.

Surahammars Bruk. 2010. Available at www.sura.se.

Szabados B., Mihalcea A. 2002. Design and implementation of a calorimetric measurement facility for determining losses in electrical machines. IEEE Transactions on Instrumentation and Measurement, Vol. 51, No. 5, October 2002, pp. 902-907.

Takenaga T., Kubota Y., Chiba A. 2002. A principle and a design of a consequent-pole bearingless motor. Proceeding of the 8th International Symposium on Magnetic Bearing, 2002, pp. 259 - 264.

Teixeira J.C., Chilled C., Yonnet J.P. 1993. Structure comparison of buried permanent magnet synchronous motors for flux weakening operation. Sixth International Conference on Electrical Machines and Drives, No. 376, 1993, pp. 365 - 370.

Tesla N. 1888. A new system of alternative current motors and transformers. Transactions on American Institute of Electrical Engineers, Vol. 5, July 1888, pp. 308-327.

Thelin P., Nee H.-P. 2000. Development and efficiency measurements of a compact 15 kW 1500 r/min integral permanent magnet synchronous motor. Conference Record of the 2000 IEEE Industry Applications Conference, Vol. 1, 2000, pp. 155-162.

Torac I. 2001. Analytical computation of magnetizing inductances for the synchronous reluctance motor with axially-laminated rotor. Workshop on Electrical Machines' Parameters, Technical University of Cluj-Napoca, 26th of May 2001.

Tsai W., Chang T. 1999. Analysis of flux leakage in a brushless permanent-magnet motor with embedded magnets. IEEE Transactions on Magnetics, Vol. 35, No. 1, January 1999, pp. 543-547.

Tseng K.J., Wee S.B. 1999. Analysis of flux distribution and core losses in interior permanent magnet motor. IEEE Transactions on Energy Conversion, Vol. 14, No. 4, December 1999, pp. 969-975.

Vagati A., Canova A., Chiampi M., Pastorelli M., Repetto M. 2000a. Design refinement of synchronous reluctance motors through finite-element analysis. IEEE Transactions on Industry Applications, Vol. 36, No. 4, July/August 2000, pp. 1094-1102.

Vagati A., Pastorelli M., Scapino F., Franceschini G. 2000b. Impact of cross saturation in synchronous reluctance motors of the transverse-laminated type. IEEE Transactions on Industry Applications, Vol. 36, No. 4, July/August 2000, pp. 1039-1046.

Yamazaki K., Fukushima Y., Sato M. 2009. Loss analysis of permanent magnet motors with concentrated windings - variation of magnet eddy - current loss due to stator and rotor shapes. IEEE Transactions on Industry Applications, Vol. 45, No. 4, July-August 2009, pp. 1334-1342.

Zaim M. 2009. High-speed solid rotor synchronous reluctance machine design and optimization. IEEE Transactions on Magnetics, Vol. 45, No. 3, March 2009, pp. 1796-1799.

Zhu W., Pekarek S., Fahimi B., Deken B.J. 2007. Investigation of force generation in a permanent magnet synchronous machine. IEEE Transactions on Energy Conversion, Vol. 22, No. 43, September 2007, pp. 557-565.

Appendices

Appendices contain Publications P1 – P8 belonging to this article dissertation.

Aalto-DD 60/2011

ISBN 978-952-60-4195-7 (pdf)
ISBN 978-952-60-4194-0
ISSN-L 1799-4934
ISSN 1799-4942 (pdf)
ISSN 1799-4934

Aalto University
School of Electrical Engineering
Department of Electrical Engineering
www.aalto.fi

BUSINESS + ECONOMY

ART + DESIGN + ARCHITECTURE

SCIENCE + TECHNOLOGY

CROSSOVER

DOCTORAL DISSERTATIONS